Chapter 7

Infrared Photodiodes on II-VI and III-V Narrow-Gap Semiconductors

Volodymyr Tetyorkin, Andriy Sukach and Andriy Tkachuk

Additional information is available at the end of the chapter

http://dx.doi.org/10.5772/52930

1. Introduction

During the last two decades HgCdTe, InSb and InAs infrared (IR) photodiodes have developed rapidly for utilization in second generation thermal-imaging systems. Obviously, they are regarded as the most important candidates for development of third generation systems as well. Despite this fact many problems still exist in manufacturing technology as well as in understanding of physical phenomena in materials and photodiodes. As a result, threshold parameters of commercially available IR photodiodes are far from the values predicted theoretically.

The concept of band gap engineering have found numerous applications in the fabrication IR devices on II-VI and V III-V semiconductors. For instance, the most important advantage of HgCdTe ternary alloy is ability to tune its energy band gap in wide range. The spectral cutoff of HgCdTe photodiodes can be tailored by adjusting the HgCdTe alloy composition over the 1-30 mm range. Further application of this concept in technology of IR detectors is closely connected with development of GaAs/AlGaAs multiple quantum well detectors and InAs/GaInSb type-II superlattice photodiodes.

To implement the concept of defect engineering, grown-in and process-induced defects must be minimized and passivated or eliminated. Defects in narrow-gap semiconductors are easily introduced either intentionally or unintentionally during crystal growth, sample treatment and device processing. There are also evidences that these defects are electrically active. So, for controlling parameters and characteristics of infrared photodiodes on narrow-gap semiconductors through defect engineering, it is essential to understand physical properties of defects, mechanisms of their interaction and temporal evolution. Electronic

properties of native defects and foreign impurities in narrow-gap semiconductors have been of great importance for several decades. As a result of intensive investigations, the primary native defects and the mechanisms of their formation were elucidated. Doping effect of different impurities has been also recognized. This allows to develop effective methods for controlling the carrier concentration and type of conductivity in intentionally undoped and doped materials. To some extent the carrier lifetime can be controlled by extrinsic doping. However, in many cases electronic states of defects in these semiconductors are still to be unknown and further investigations are needed.

For controlling properties of semiconductors through defect engineering, it is essential to understand the mechanisms of interaction between point and extended defects (dislocations), as well as to understand their effect on device characteristics. This task seems to be important since alternative substrates (Si, GaAs, sapphire) are widely used in epitaxial technology of IR photodiodes. These substrates are very attractive because they are less expensive and available in large area wafers. The coupling of the Si substrates with Si read-out integrated circuit allows fabrication of very large focal-plane arrays (FPA). Due to the large lattice mismatch between HgCdTe, InSb and InAs and alternative substrates, photodiodes on their base suffer from the high density of dislocations (typically of the order of 10^6 cm^{-2}). For instance, these defect densities seriously limit application of HgCdTe epitaxial layers for manufacture of high-performance photodiodes for the LWIR and VLWIR spectral regions. The use of buffer layers, temperature cycling and hydrogen passivation is expected to be useful for reduction of the density of dislocations and weakening their effect on the device performance. However, none of these methods has yet been proven to be practical.

A number of physical properties of HgCdTe, such as direct energy gap, ability to obtain both low and high carrier concentrations, high mobility of electrons and holes, low dielectric constant and extremely small change of lattice constant with composition, makes it possible to grow high quality layers and heterostructures. As a consequence, high-performance HgCdTe photodiodes on mead-wavelength, long-wavelength and very long-wavelength IR regions (MWIR, LWIR and VLWIR) have been developed. The main drawbacks of HgCdTe are technological disadvantages of this material. The most important is a weak Hg–Te bond, which results in bulk, surface and interface instabilities. Uniformity and yield are still issues especially in photodiodes on the LWIR and VLWIR spectral regions. InSb photodiodes on the MWIR spectral region have comparable performance with photodiodes made of HgCdTe.

Initially, the IR photodiodes were prepared by diffusion, ion implantation or other techniques which allow preparation of homojunction structures. In these photodiodes, the concentration of carriers in the lightly doped ‘base’ region was strongly controlled. With development of epitaxial techniques, homojunction photodiodes were replaced by heterojunction ones. In a heterojunction photodiode the ‘base’ region are introduced between a wide-gap substrate and a capping layer with wider band gap. Thus, the influence of surface recombinations on the photodiodes performance is weakened. It seems that the most successful application of the band gap and defect engineering concepts in technology of IR photodiodes is development of double-layer heterojunction photodiodes.

http://dx.doi.org/10.5772/52930

The main objective of this article is to outline the basic properties of point and extended defects, their effect on physical properties and threshold parameters of infrared photodiodes based on HgCdTe, InAs and InSb narrow-gap semiconductors. This article is divided into two parts. The first part is dedicated to technological steps (crystal growth, thermal annealing, junction formation) closely connected with defects forming in materials and devices. In the second part original results are analyzed with emphasize on possible participation of dislocations and point defects in the carrier transport mechanisms and recombination processes in the photodiodes.

2. Native defects and impurities in HgCdTe, InAs and InSb

The defect structure of narrow-gap $Hg_{1-x}Cd_xTe$ (hereinafter – HgCdTe) compounds was intensively investigated both theoretically and experimentally over the past fifty years. The current status of defect states in these semiconductors are reviewed in numerous papers and monographs (see, e.g., Capper and Garland, 2011; Chu and Sher, 2010). HgCdTe crystalline materials are always grown with large deviation from stoichiometry. The equilibrium existence region in HgCdTe (x~0.2) is shown to be completely on the Te-rich side (Schaake, 1985). Thus, the most important type of native point defects in undoped materials are Hg vacancies. Residual impurities, Hg interstitials, dislocations and Te precipitates were also observed in as-grown materials. All these defects can exist in neutral or ionized states. Their important characteristics, such as donor or acceptor type, ionization energy, density, spatial location and temporal variation were investigated.

The ab initio calculation of the formation energies of native point defects in HgCdTe (x~0.2) has been made by Berding with co-authors (Berding, 1994, 1995, 2011). The most reliable calculations are based on the local-density approximation to the density functional theory. The calculations predict the mercury vacancy and the tellurium antisite Te_{Hg} as the dominant defects in the material grown under tellurium-rich conditions. The concentration of native point defects was calculated as a function of Hg pressure using quasichemical formalism. In the the calculation all defects were assumed to be equilibrated at the temperature 500 0C and the defect concentrations were assumed to be frozen in. The 500 ^{0}C temperature is typical of LPE growth. In the calculations the Hg vacancy and tellurium antisite Te_{Hg} are classified as acceptor and donor defects, respectively. The calculation also predicts that the concentration of Te_{Hg} is comparable with the mercury vacancies concentration. At the same time, as was pointed by Berding, to date there is no experimental confirmation of the presence of the tellurium antisite defects in HgCdTe in so large amounts. Also, the calculated concentration of Hg interstitial was found to be too low to explain experimental data on the self diffusion (Berding, 2011). Experimentally the defect structure in undoped HgCdTe (x~0.2) was investigated by Vydyanath and Schaake. It has been shown that the dominant native defects are doubly ionized acceptors associated with Hg vacancies (Vydyanath, 1981; Schaake, 1985). This result is in accordance with the theoretical prediction. Defects in doped HgCdTe have been reviewed by Shaw and Capper (Shaw and Capper, 2011).

Native defects in HgCdTe, including dislocations and defect complexes, can act as Shockley-Read-Hall (SRH) centers due to their effect on the carrier lifetime. There is a large literature concerning the links of deep defects to the carrier lifetime in HgCdTe (Capper, 1991; Sher, 1991; Capper, 2011; Cheung, 1985, Chu and Sher, 2010). Clear evidence of SRH centers was provided by deep level transient spectroscopy, admittance spectroscopy, thermally stimulated current and optical modulation spectroscopy (Polla, 1981, 1981a, 1981b, 1982; Jones, 1982; Schaake, 1983; Mroczkowski, 1981). The centers located at near midgap seems to be common to p-type Hg_iCdTe, where the doping is due to mercury vacancies. Summary of impurity and native defect levels experimentally observed in HgCdTe has been done by Litter et. al. (Litter, 1990). The main results of experimental findings are as follows: (i) shallow acceptor-like levels have activation energies between 2 and 20 meV; deep levels have energies $0.25E_g$, $0.5E_g$ and $0.75E_g$ above the valence band edge. The concentration of donor-like deep centers reported by Polla and co-authors was ranged from approximately $0.1N_A$ to $10N_A$, where N_A is the shallow acceptor concentration. The values of the cross section for electrons and holes were in the range 10^{-15}-10^{-16} cm^2 and 10^{-17}-10^{-18} cm^2, respectively. The origin of the SRH centres in HgCdTe is still not clear. The vacancy-doped materials with approximately the same carrier concentration, but manufactured at different temperature conditions, may exhibit different lifetimes. At the same time, the correlation has been found between the SRH recombination centre densities and the Hg vacancies concentration (Capper, 2011).

The behavior of extrinsic defects in HgCdTe is important from several reasons. Manufacture of photodiodes with improved characteristics requires intentionally doped materials with controllable concentrations of acceptors and donors instead of vacancies-doped material. This is caused by several reasons such as instability of the vacancy-doped material and low ability to control the concentration of free carriers. Also, Hg vacancies or complexes with their participation may be responsible not only for the carrier lifetime, but also they can enhance the trap-assisted tunneling, giving rise to excess dark current in infrared photodiodes. Shaw and Capper (Shaw and Capper, 2011) provides a complete summary of the work on dopants in bulk material and epitaxial layers. Indium and iodine are most frequently used as a well-controlled donors for preparation of n-type bulk material and epitaxial layers. Both are incorporated as shallow single donors occupying metal and tellurium lattice sites (In and I, respectively). Indium has moderately high diffusivity whereas diffusivity of iodine is rather low. Group V elements have low diffusivity and hence are ideal as p-type dopants. Approximately 100% activity is found for In and I concentrations up to ~10^{18} cm^{-3}. Vydyanath (1991) argued that group V elements (P, As, Sb, Bi) are incorporated as donors under Te-rich (Hg-deficient) conditions of growth. Under Hg saturated anneal at 500 ^{0}C there is enough energy to move these elements from metal lattice cites to Te or interstitial sites. The group V impurities if occupy Te sites act as shallow acceptors.

Shallow impurities are known to determine the concentration of free carriers in semiconductors. The ionization energy of a hydrogen-like donors in HgCdTe were calculated as a function of composition and concentration of defects (Capper, 2011). Due to low effective masses of electrons this energy is too small to be detected experimentally at 77 K (e.g., the ionization energy is 0.30 (0.85) meV for the composition x=0.2 (0.3). The ionization energy for acceptors

http://dx.doi.org/10.5772/52930

depends on the material composition, concentration of acceptors and degree of compensation. The calculated energy for the shallow acceptors is 11(14) meV for x=0.20 (0.3).

Electronic properties of extended defects in HgCdTe, InSb and InAs are less investigated in comparison with point defects. It is known that II-VI semiconductors are more ionically bonded as III-V covalent semiconductors. As a result, they can be easily plastically deformed at room and lower temperatures (Holt and Yacobi, 2007). The photoplastic effect, discovered by Osipiyan and Savchenko (1968), is conclusive proof that dislocations in II-VI materials are electrically charged and that charge is largely electronically determined. The dislocation core contains broken bonds so the dislocation line may generally be charged negatively. The broken bonds are chemically reactive and electrostatic interaction between the charged dislocation lines and ionized point defects and short-range chemical bonding effects may occur. This tends to reduce (neutralize or passivate) the electrical effects of dislocations especially in the ionically bonded II-VI compounds. The charge states of the dislocation can be altered illumination and other means of carrier injection and this can change dislocation line charges as well as dislocation mobility. Yonenaga (1998) compared the dynamics of dislocations in InAs with those in other semiconductors, including narrow-gap and wide-gap II-VI compounds. It has been shown that the activation energies for dislocation motion depend linearly on the band-gap with an apparent distinction between different types of semiconductors. The activation energy is lower in ionically bonded II-VI semiconductors compare to III-Vs. Thus, dislocations would be expected to be the most mobile in II-VI narrow-gap semiconductors. The long-range electrostatic interaction strengthens the attraction of dislocations to their Cottrell impurity atmospheres and strengthens the pinning effect opposing dislocation motion.

Dislocations can also act as SRH centers in HgCdTe and III-V narrow-gap semiconductors. The electrical activity of dislocations can be attributed to Cottrell atmosphere, or to dangling bonds in the dislocation core. The ability of the strain fields of dislocations in HgCdTe to capture significant amounts of impurities has been investigated in the early work by Schaake (Schaake, 1983). It has been argued that the origin of the electrical activity is dangling bond states on the dislocations rather that the impurities. The high Peierls stress observed in II-VI compound semiconductors supports this argument. This stress has been attributed to the ability of dangling bonds to heal themselves along the dislocation core. The reduced lifetime and mobility caused by dislocations in n- and p-type HgCdTe has been pointed out in several papers (Lopes, 1993; Yamamoto, 1985; Shin, 1991). This reduction has been ascribed to dangling bonds which provide SRH centers. Dislocations also affect the dark currents in LWIR photodiodes operating at low temperatures (<77 K) because they are believed to produce mid-gap states in the band gap (Arias, 1989; Tregilgas, 1988). The decrease of the differential resistance-area product at zero bias voltage, R_0A, in the presence of high dislocations densities has been reported by Johnson et al. (Johnson, 1992). As the temperature decreases the effect of dislocations was found to be more significant. At 77 K the decrease of R_0A begins at the dislocation density of the order of 10^6 cm^{-2}, whereas at 40 K it is affected by the presence of one or more dislocations. The scatter in the R_0A data may be associated with the presence of pairs of 'interacting' dislocations, which may be more effec-

tive in reducing the R_0A than individual dislocations. The excess current in photodiodes caused by dislocations may be the source of 1/*f* noise.

The effect of misfit dislocations on dark currents in high temperature MOCVD HgCdTe infrared heterostructure photodiodes has been investigated by Jóźwikowska et al. (Jóźwikowska, 2004). It was shown that the most effective current transport mechanism at high temperature in HgCdTe heterostructures is the trap-assistant tunneling. In the photodiodes operated at 240 K, this mechanism is predominant at bias voltage that not exceeded 0.1 V. The best fit of experimental data with theoretical predictions for the zero bias differential resistance versus temperature has been obtained for rather high dislocation densities in the volume of HgCdTe layer ~5 10^7 cm-^{2}. To a certain extent electrical activity of dislocation can be reduced by passivation (Boieriu, 2006). It has been showed that incorporation of H in In-doped HgCdTe (x = 0.2) epilayers, through exposure to an electron cyclotron resonance (ECR) H plasma, the lifetime increases by a factor of 10. The increase was attributed to H passivation of the dangling bonds and is only effective for high dislocation densities (~10^7 cm^{-2}).

The early studies of native defects and impurities in InSb and InAs have been summarized by Milnes (Milnes, 1973). The energy of shallow impurities in InAs and InSb was calculated with extension of effective mass theory (Baldereschi and Lipari, 1974). Several deep donors of undetermined origin have been observed in InSb. Copper atoms segregated at dislocations in InAs are apparently electrically inactive, but on heating they diffuse away and can be frozen into the lattice as electrically active centers. They return to the dislocations during the low-temperature anneal. A similar effect was observed with Cu in InSb. A number of undetermined deep defects was found in InSb and InAs (Madelung, 2003).

The nature of intrinsic point defects in InAs single crystals has been studied by several groups (Bublik, 1977, 1979, 1979a; Karataev, 1977; Mahony and Maseher, 1977). In specially undoped InAs single crystals grown by direct solidification and Czochralski methods precision measurement of density and lattice constant has been made in order to determine the type and concentration of interstitial atoms and vacancies depending on the content of arsenic in InAs melt. The difference in concentrations of V_{As} and As_i for InAs was found to be of the order of 3 10^{18} cm^{-3}. For InAs grown from the melt of stoichiometric composition, this difference does not exceed $1{\cdot}10^{17}$ cm^{-3}. It was also established the effect of point defects on structural and recombination properties of InAs single crystals. It is shown that InAs crystals were n-type conductivity and electron concentration increased from $1.4{\cdot}10^{16}$ to $2.5{\cdot}10^{16}$ cm^{-3} (T = 77 K) with increasing of As content in the growth melt. It has been concluded that the concentration of electrons is determined by intrinsic defects and complexes composed of native defects (vacancies) and background impurities. The effect of annealing on electrical properties of undoped indium arsenide has been investigated by Karataev (1977). The annealing was made in the temperature range 300-900 °C for 1-100 h. It was found that the annealing increases the concentration of electrons. For example, for the annealing temperature ~900 °C the concentration of electrons increased from $2{\cdot}10^{16}$ cm^{-3} to $2{\cdot}10^{17}$ cm^{-3}.

http://dx.doi.org/10.5772/52930

Impurity, structural defect	Type	Ionization energy, meV	Concentration, cm^{-3}	Reference
As divacancy+ residual impurity	neutral complex	-	$(7 \pm 2)\cdot10^{16}$	Mahony, J. and Maseher, P., 1977
As monovacancy+ residual impurity	neutral complex	-	$\sim 1\cdot10^{17}$	Mahony, J. and Maseher, P., 1977
V_{In}	A_1	E_V+100	-	Mahony, J. and Maseher, P., 1977
V_{In}	A_2	E_V+130	-	Mahony, J. and Maseher, P., 1977
V_{In}	A_3	E_V+230	-	Mahony, J. and Maseher, P., 1977
V_{As}	D	$E_C+0.03E_g$	-	Bynin, M.A. and Matveev, Yu.A., 1985
V_{As}	D	E_C-$E_g/4$	-	Bynin, M.A. and Matveev, Yu.A., 1985
Cr	D	E_C–160	-	Omel'yanovskii,1975; Balagurov, 1977; Plitnikas,1982; Adomaytis,1984
S, Se, Te	D	E_C– (2–3)	-	Voronina, 1999
Mn	A	E_V + (28-30)	-	Adrianov, 1977; 26 Gheorghitse,1989
Zn	A	E_V+10	-	Kesamanly, 1968
Zn	A	E_V +25	-	Guseinov, 1969; Guseinov, 1997
Cd	A	E_V+20	-	Galkina, 1966
Cd	A	E_V+11	-	Iglitsyn, 1968
Mg	A	-	-	Voronina, 2004
Cu	D	E_C-< 7	-	Karataev, 1977
Pb	N	-	-	Baranov, 1992; Baranov, 1993
Be	A	E_V+< 7	-	Lin, 1997; Astahov, 1992; Dobbelaere, 1992
Ge (amphoteric)	D (Ge sub.In)	E_C-< 7	-	Guseva, 1974; Guseva, 1975
Ge (amphoteric)	A (Ge sub. As)	E_V+14	-	Guseva, 1974; Guseva, 1975
Si (amphoteric)	D (Si sub. In)	E_C-< 7	-	Guseva, 1974; Guseva, 1975
Si (amphoteric)	A (Si sub. As)	E_V+20	-	Guseva, 1974; Guseva, 1975
Structural defect	-	110±20	$(0.5\div10)\cdot10^{14}$	Fomin, 1984
-	-	150±20	$\leq 5\cdot10^{14}$	Fomin, 1984
-	-	~ 220	$(1\div3)\cdot10^{15}$	Ilyenkov, 1992
-	-	~$E_g/2$ (77 K)	$\sim 10^{17}$	Kornyushkin, 1996
-	D	E_C–(100-200)	-	Baranov, 1992
-	D	E_C–(10-20)	-	Baranov, 1992
-	A	E_V+50	-	Baranov, 1992
-	D	E_C–15	-	Baranov, 1993
-	A	E_V+50	-	Baranov, 1993
-	D	E_C– (20-30)	-	Voronina, 1999
-	D	E_C–(90-100)	-	Voronina, 1999
-	A	E_V+10	-	Voronina, 1999a
-	A	E_V+20	-	Voronina, 1999a
-	A	E_V+30	-	Voronina, 1999a
-	A	E_V+65	-	Voronina, 1999a
-	A	E_V+20	-	Zotova, 1975
-	A	E_V+35	-	Zotova, 1975
-	A	E_V+35	-	Allaberenov, 1970
-	A	E_V+35	-	Esina, 1985
Residual impurity	D	E_C–2	-	Baranov, 1992
Dislocation (possibly)	A	E_V+(45-50)	-	Anisimova, 1969

Table 1. Parameters of impurities and structural defects in InAs

Impurity, structural defect	Type	Ionization energy, meV	Concentration, cm^{-3}	Reference
Zn	A	$E_V + 8$	-	Ismailov, 1969
Zn	A	$E_V + 10$	-	Pehek and Levinstein, 1965
Ge	A	E_V+ (16-19)	-	Ismailov, 1969
Ag_1	A_1	E_V+27	-	Pehek and Levinstein, 1965
Ag_2	A_2	E_V+50	-	Pehek and Levinstein, 1965
Au	A	E_V+43	-	Pehek and Levinstein, 1965
Cu	A	E_V+ (57-64)	-	Valyashko, 1975
Cu	A	E_V+(23-27)		Kevorkov, 1980
Cu, Ag, Au	A	E_V+67	$3 \cdot 10^{14}$	Korotin, 1976
Structural defect	D	E_C–48	-	Valyashko, 1975
-	A	E_V+ (7-9)	$\leq 6 \cdot 10^{14}$	Kevorkov, 1980
-	A	E_V+ (5-6)	-	Nasledov, 1962
-	D	E_C– (7-8)	-	Nasledov, 1962
-	D	E_C–55	$\sim 8 \cdot 10^{13}$	Laff and Fan, 1961
-	D	E_C–60	10^{11} - 10^{13}	Sipovskaya and Smetannikova, 1984
-	A	E_V+ (50-60)	$\sim 10^{14}$	Zitter, 1959
-	D	E_C- (65 ± 5)	$(1.3 - 7.5) \cdot 10^{13}$	Golovanov, 1973
-	A	E_V+ (20-30)	$1 \cdot 10^{15}$	Guseinov, 1971
-	D	E_C–110	-	Valyashko, 1975
-	A	E_V+ (150-170)	$(0.3\text{-}1.0)\ 10^{12}$	Tsitsin, 1975
-	D	E_C– (50-70)	-	Trifonov, 1971
-	A	E_V+ 120	-	Golovanov, and Oding, 1969
-	D	E_C– (110-120)	$< 7 \cdot 10^{13}$	Nasledov, 1962
-	D	E_C–120	$\sim 8 \cdot 10^{13}$	Laff and Fan, 1961
-	D	E_C–140	$\sim 2 \cdot 10^{14}$	Volkov and Golovanov, 1967
-	D	E_C–110	$\sim 3 \cdot 10^{13}$	Hollis, 1967
-	D	E_C–71	$\sim 3 \cdot 10^{13}$	Hollis, 1967
-	A	E_V+ (60-63)	-	Egemberdieva, 1982
-	A	E_V+ (69-73)	-	Egemberdieva, 1982
-	A	E_V+ (80-82)	-	Egemberdieva, 1982
-	D	E_V+ (110-113)	-	Egemberdieva, 1982
-	D	E_V+ (131-135)	-	Egemberdieva, 1982
-	D	E_V+ (140-142)	-	Egemberdieva, 1982
-	D	E_C–130	10^{13} - $2 \cdot 10^{15}$	Sipovskaya and Smetannikova, 1984
-	-	E_V+ (120±30)	$(0.7 - 2.3) \cdot 10^{15}$	Golovanov, 1973
-	-	E_C–130	$\sim 1.2 \cdot 10^{14}$	Korotin, 1976
-	-	E_C–220	$(2 - 5) \cdot 10^{12}$	Korotin, 1976
-	-	E_C–110	$2 \cdot 10^{14}$	Guseinov, 1971
-	A	E_V+68	$(3 - 4) \cdot 10^{13}$	Shepelina and Novototsky-Vlasov, 1992
-	D	E_V+99	$(6 - 8) \cdot 10^{13}$	Shepelina and Novototsky-Vlasov, 1992
-	D	E_V+132	$(2 - 3) \cdot 10^{13}$	Shepelina and Novototsky-Vlasov, 1992
In_i+O_2	A	E_C-50		Zaitov, 1981

a. in Table 1 and 2 residual impurities and structural defects have unknown identity;

b. doping behavior is indicated by A, acceptor, D, donor; A_1,A_2 and A_3 means singly, doubly and triple ionized acceptor.

Table 2. Parameters of impurities and structural defects in InSb[a,b]

http://dx.doi.org/10.5772/52930

The greatest effect of the anneal was observed in InAs, grown from the melt with an excess of indium or arsenic atoms. Dislocations with densities from 10^3 to 10^5 cm^{-2} were found to contribute to the effective change in the concentration of electrons at the annealing process. Investigation of defect complexes in InAs using positron annihilation has been presented by Mahony and Maseher (1977). The neutral complexes with the concentration of $(7\pm2)\bullet10^{16}$ cm^{-3} has been found. Moreover, these complexes are composed of two vacancies at high temperatures whereas at low temperatures only one vacancy is participated in a complex. Both complexes are stable up to temperatures ~850 ^{o}C. Theoretical calculations of energy levels related with In and As vacancies was also carried out (Mahony and Maseher, 1977). It is shown that In and As vacancies are acceptors and donors, respectively. Growing the high resistivity InAs LPE films doped with chromium and study its electrical and photovoltaic properties was also reported (Omel'yanovskii,1975; Balagurov, 1977; Plitnikas,1982; Adomaytis,1984). Based on investigations of deep centers in epitaxial layers of InAs, the development of high-quality MOS-structures with a density of surface states ≤2 10^{10} cm^{-2} eV^{-1} has been realized. Linear and matrix IR photodetector hybrid assemblies with the temperature resolution of 4 - 8 mK were prepared (Kuryshev, 2001, 2009).

The deviation from the stoichiometry in InSb has been investigated by Abaeva et al. (Abaeva, 1987). The authors make a precise determination of the temperature dependence of the InSb lattice constant by Bond's method. It is shown that In and Sb vacancies are the principal intrinsic point defects that determine the deviation from stoichiometry in InSb and reduce the lattice constant. The mid-gap defect states were observed in InSb bulk crystals (Ehemberdyeva, 1982; Shepelyna, 1992). Their energy does not depend on the chemical nature of dopant and the doping level. Defect complex composed of indium and oxygen atoms with energy E_C-50 meV has been found by Zaitov et al. (Zaitov, 1981). The low temperature (~200 ^{0}C) annealing in an atmosphere of inert gas or saturated vapor of lead results in 5-10 times increasing of the carrier lifetime in n-InSb (Tsitsina,1975; Strelnikova, 1993). A model of the conductivity type conversion with participation of fluorine has been proposed (Blaut-Blachev,1979; Kevorkov, 1980). Some parameters of impurities and deep defects in InAs and InSb are summarized in Table. 1 and 2.

3. Defect-related manufacturing processes

3.1. Growth techniques

Various methods have been proposed for growing II-VI and III-V semiconductor crystals. These methods can be roughly classified into the melt growth, solution and vapor growth methods. Each of the proposed growth methods has its own advantages and disadvantages. For growing II-VI semiconductor compounds there exist a problem of high dissociation pressure which leads to evaporation of a volatile component and hence deviation from stoichiometry. The deviation from stoichiometry introduces lattice defects since there is a deficiency of one component. If there is a large deviation from stoichiometry, vacancies can combine with the residual impurities or with the impurities which are later introduced into

the crystal during a subsequent process. The number of defects is hard to control in this case. Therefore, from the point of perfect crystallography, it is desirable to grow crystals at temperatures as low as possible. This requirement is especially important for HgCdTe alloys, since they are decomposing solids. Also, the liquidus-solidus temperatures of the mercury telluride and cadmium telluride compounds are different, which causes their segregation as the alloy is frozen from a melt. The resultant variation of the mole fraction of each compounds results in a consequent variation in energy gap as well as electrical and optical properties throughout the material. In contrast to HgCdTe, the III-V compounds (InSb and InAs) melt congruently, i.e. a liquid and solid having identical compositions are in equilibrium at the melting point. Thus, they can be grown directly from the melt, a process commonly used to grow large boules of InAs and InSb.

Further progress in IR photodiode technology is connected with epitaxial layers. Epitaxial techniques offer the possibility of growing large area layers with good depth and lateral homogeneity, abrupt composition and doping profiles, which can be configured to improve the performance of photodiodes. The commonly used methods for preparation of epitaxial films are liquid phase epitaxy (LPE), molecular beam epitaxy (MBE), metal-organic vapor phase epitaxy (MOVPE), and metal-organic chemical vapor epitaxy (MOCVD). LPE method is a near-thermodynamic equilibrium growth technology. It has the advantages of relatively simple process, high utilization rate of the source material, high crystalline quality of the epitaxial films and fast growing. The weakness of LEP is that it cannot be used for precision controlled growth of very thin films of nano-scale. In other words, it is not applicable to the growth of superlattices or quantum-well devices and other complex micro-structure materials. In addition, the morphology of materials grown by LPE is usually worse than that grown by MOCVD or MBE. In these techniques epitaxial growth is performed at low temperatures, which makes it possible to reduce the native defects density. Obviously, for epilayers the choice of substrate is decisive for minimizing effect of misfit dislocations and interdiffusion at the epilayer/substrate heterojunction. This problem is especially important for InSb and InAs because of the lack of lattice-matched III-V wide-gap semiconductors which may be used as substrates. To overcome this difficulty, the use of alternative substrates (Si, GaAs, supphire) attracts great attention. Successful implementation of epitaxy of narrow-gap semiconductors on Si substrates can directly lead to possibility of realization of multicolor, monolithic focal plane arrays.

3.1.1. Growth of HgCdTe

Several historical reviews of the development of bulk HgCdTe have been published (Maier and Hesse, 1980; Capper, 1994; Capper, 1997). Bulk growth of HgCdTe is rather difficult due to the high vapor pressure of Hg at the crystal melting point (about 950 ^{0}C), caused by weak Hg-Te bond in a crystal. For bulk material the Bridgman, solid state recrystallization, and travelling heater methods have been developed. The most successful implementation of the bulk growth technique was the travelling heater method which allows to grow up to 5-cm diameter single crystals of high structural and electrical quality. Bulk crystal growth is currently used to support the first generation of photoconductive HgCdTe array fabrication.

http://dx.doi.org/10.5772/52930

The LPE is the most matured method for preparation of high-quality HgCdTe epitaxial films (Capper, 2011). Two different approaches have been developed: growth from Te and Hg solutions at 420-600 ^{0}C and 380-500 ^{0}C, respectively. Dipping, tipping and sliding boat techniques have been used to grow both thin and thick films. The tipping and dipping techniques have been implemented by using both tellurium- and mercury-rich solutions, but only tellurium-rich solutions have been used with the sliding boat. Both Hg- and Te-rich LPE can produce material of excellent compositional uniformity and crystalline quality (Capper, 2011).

MBE and MOVPE growth of HgCdTe is performed at much lower temperatures compare to LPE. Growth temperature is typically around 200-350 ^{0}C in MOVPE and around 150-200 ^{0}C in MBE (Garland, 2011; Maxey, 2011). Due to the weak Hg-Te bond, the evaporation of this material is not congruent. Consequently, Hg re-evaporates from the growth surface, leaving the surface Hg-deficient. Because of a large flux of Hg is necessary in this case, it means that the MBE growth temperature window is extremely small for HgCdTe and precise control of the growth temperature is highly desirable (Arias, 1994; Arias, 1994a). Furthermore, to obtain a desired cut-off wavelength within ±6%, one must control the Cd composition x within ±0.002 (Garland, 2011).

Routinely produced CdTe and CdZnTe (Zn~ 3-4%) single crystals are used as substrates for MBE and MOVPE growth. Today, the largest commercially available CdZnTe substrates are limited to approximately 7x7 cm^2 area. At this size, the wafers are unable to accommodate more than two 1024x1024 FPAs (Rogalski, 2009). Also, the quality of epitaxial layers is influenced by poor thermal conductivity, compositional nonuniformity, native defects, surface roughness and imperfect surface flatness CdZnTe substrates.

The most used dopants for MBE and MOVPE growth are arsenic as the p-type dopant and indium and iodine as the n-type dopants. There are no problems with in-situ incorporation of indium and iodine and low-temperature post-growth annealing is used to optimize the structural and electronic properties of the doped material, but is not required for activation of dopants. The MBE growth of HgCdTe is optimally performed under Te-rich conditions (Arias, 1994), thus Hg vacancies are the dominant native point defects in as-grown layers. Due to this reason the in-situ incorporated As occupy Hg sites in a lattice and annealing is required to its activate as a p-dopant by transferring to Te sites. The standard activation anneal is 10 min at ~425 ^{0}C followed by 24h at ~250 ^{0}C under a Hg overpressure to fill the Hg vacancies. The high-temperature annealing it limits many of the low-temperature-growth advantages of MBE. Therefore, attempts have been made to obtain the p-type activation of As either as-grown or after only a low-temperature anneal (Garland, 2011).

The use of alternative Si and GaAs substrates are attractive in IR FPA technology due to several reasons including available Si substrates with large sizes (up to 300 mm diameter), lower cost and compatibility with semiconductor processing equipment. The match of the coefficient of thermal expansion with Si readout circuit allows fabrication of very large FPAs exhibiting long-term thermal cycle stability. Of course, the large lattice mismatch between HgCdTe and alternative substrates (Si: 19%, GaAs: 14%) causes a high dislocation density (typically from mid-10^6 to mid-10^7 cm^{-2}) at the epilayer/substrate interface due to propagating of dislocations in the growth direction. The high dislocation density is detrimental to de-

vice performance because of the effect of dislocations on minority carrier lifetimes (Shin, 1992). For comparison, in epitaxial layers grown on CdTe and CdZnTe substrates the dislocation density is less than mid-10^5 cm^{-2}. The dislocation density below this value is believed to be not a serious problem unless they form clusters under device contacts. Despite these difficulties, epitaxial growth of high quality HgCdTe on 4-inch CdTe/Si substrates has been demonstrated for MWIR applications (Maranowski, 2001). Also, large area high quality HgCdTe epilayers were grown by MBE on 100 mm diameter (211)Si substrates with a CdTe/ZnTe buffer layer (Bornfreund, 2007). Epilayers of HgCdTe with extremely uniform composition and extremely low defects density were demonstrated by Peterson et al. (Peterson, 2006) on 4- and 6-inch diameter silicon substrates.

The lattice matched and alternative substrates with (100) and (211) orientations are commonly used. The best crystalline quality is obtained on the substrates with the slightly misoriented surfaces. For instance, the MOVPE growth on (100) substrates misoriented from the (100) plane by a few degrees is useful to suppress the formation of pyramid-shaped macrodefects, known as hillocks (Maxey, 2011). Today almost all growth is carried out on (211) substrates, which have (111) terraces with (100) steps (Garland and Sporken, 2011).

The MBE and MOVPE technology of HgCdTe has developed to rather high level at which epitaxial layers grown on bulk CdTe and CdZnTe substrates have characteristics comparable to those of LPE material.

3.1.2. Growth of InSb and InAs

Due to the relatively low melting point of (525 ^{0}C) and small saturation vapor pressure, InSb bulk crystals can be grown using different growth techniques: Czochralski and horizontal Bridgman technique, travelling heater method and zone melting (Hulme and Mullin, 1962; Liang, 1966; Parker, 1965; Benz and Müller, 1975; Bagai, 1983). Technology of InSb bulk crystals are well matured. InSb is the most perfect material among the III-V semiconductors available to data. Typically 10-100 cm^{-2} etch pit density is specified in a commercially available InSb. However, the best result is only 1 etch pit in 50 cm^{-2}. In the ultra-high pure InSb bulk crystals the carrier concentration can be lower 10^{13} cm^{-3}.

In contrast to indium antimonide, InAs possesses an appreciable vapor pressure at the melting point (943 ^{0}C), because of the equilibrium vapor is constituted of the more volatile component (As) whose condensation and sublimation temperature lies below the melting point. However, even at this case, there is a strong tendency to form stoichiometric compound. InAs bulk crystals can be grown using liquid covering Czochralski or vertical gradient freeze method. Because of purification of InAs is more difficult than InSb, the residual electron concentration of InAs bulk crystals is about of $2{\cdot}10^{16}$ cm^{-3}.

Gettering effect of lead and rare earth elements (ytterbium and gadolinium) in LPE of InAs has been studied by several groups (Baranov, 1992, 1993; Voronina, 1999; Gao, 1999). The gettering effect of lead is attributed to the formation of stable insoluble aggregates composed of indium tellurides, selenides and sulphides. As a result, epitaxial films with the concentration of electrons $\sim^{15}$ cm^{-3} and mobility 9.1 10^4 cm^2/V s at 77 K have been grown. In

http://dx.doi.org/10.5772/52930

these films reduction of the concentration of structural defects was also observed. The simultaneous introduction of controlled amounts of lead and rare earth elements makes it possible to prepare high resistivity films with the compensation degree 0.6-0.9. In the compensated films the electron concentration $3 \cdot 10^{15}$ cm^{-3} was achieved. The defect complexes of n-type were also observed in these films.

Various efforts have been made to adopt LPE growth of InSb (Kumagava, 1973; Mengailis, 1966; Holmes, 1980). However, there is a small number of reports on successful growth of InSb films by this method. Recently Dixit and co-authors reported growth of high-quality films on (001) semi-insulating GaAs substrate in a boat-slider type LPE unit (Dixit, 2002; Dixit, 2002a).

Heteroepitaxy of InSb and InAs has been achieved on Si and GaAs substrates with MBE and MOCVD technology (Razeghi, 2003). To overcome the lattice mismatch (>19%), the MBE of InSb on Si substrates was performed using CaF_2 and stacked BaF_2/CaF_2 buffer layers. The room temperature electron mobility of 65000 cm^2/V s ($n \approx 2\ 10^{16}$ cm^{-3}) was obtained in an 8 μm-thick film grown on a Si substrate with 0.3 μm CaF_2 buffer layer. The 77 K mobilities were at least an order of magnitude lower than the room temperature values. This behavior of electron mobility is attributed to electron scattering on dislocations arising from both lattice and thermal strains (Liu, 1997).

Epitaxial layers of InSb were grown directly on InSb, GaAs and GaAs-coated Si substrates with MBE and a low pressure MOCVD techniques (Razeghi, 2003). The quality of epitaxial films has been shown to depend critically on the growth conditions and preparation of substrates. In order to get high crystal quality InSb and GaAs substrates, directed 2^0 off the (100) toward (110) direction were used. The X-ray rocking curve FWHM, electron concentration and mobility was found to depend on the thickness of films due to influence of highly dislocated interface. In 3.6 μm thick InSb film the electron mobility was 56000 $cm^2/V \cdot s$ at 300 K and close to 80000 $cm^2/V \cdot s$ at 77 K. The background electron concentration at 77 K was of the order of 10^{16} cm^{-3}. Excellent uniformity (within the ±3 arcs variation of FWHM) was detected for a 10 μm thick InSb layer grown by MBE on a 3-inch semi-insulating GaAs substrate. The FWHM decreases with thickness as the dislocation density decreases due to the greater distance between the surface and the highly dislocated interface. The 300 K mobility close to that of bulk InSb (75000 $cm^2/V \cdot s$) was achieved in the films with thickness more than 2 μm. The temperature dependence of the electron mobility was peaked at 77 K and decreased at lower temperatures due to the dislocation scattering at the InSb/GaAs interface (Razeghi, 2003).

The MBE growth of InAs has been reported by several groups (Yano, 1997; Kalem, 1998). InAs epitaxial layers with thicknesses ranging from 0.5 up to 6.2 μm was grown on (100) oriented semi-insulating GaAs substrates. As in the case of InSb films, the properties of InAs films was influenced by the growth conditions and InAs/GaAs interface structure. The electron mobility at room temperature is $1.8\ 10^4$ $cm^2/V \cdot s$ ($n=6.1\ 10^{15}$ cm^{-3}) and peaks at about liquid-nitrogen temperature with a value of $5.173\ 10^4$ $cm^2/V \cdot s$ ($n=3.1\ 10^{15}$ cm^{-3}) for a InAs layer with thickness of 6.2 μm. It is shown that the temperature dependence as well as the magnitude of the mobility can be explained by a combined impurity-phonon-dislocation scattering

mechanism. The dislocation densities of the order of 10^6 cm^{-2} were found. High-quality InAs epilayers on the GaAs substrates have been grown by MBE (Chen,2000; Cai, 2003). The growth was carried out as a two-step process: InAs layers were grown under As-rich conditions on InAs prelayers grown directly on the GaAs substrates under In-rich conditions. The optimized growth condition for this method from the Raman spectroscopy and the low-temperature photoluminescence was the following: first InAs is grown 20 nm thick under In-rich conditions at 500 ^{0}C with the appropriate V/III ratio of 8, then InAs is continuously grown under As-rich conditions at 500 ^{0}C with the appropriate V/III ratio of 10–23. Also, a two-step growth method consisting of a 400 ^{0}C prelayer followed by deposition of the thick bulk layer at higher growth temperatures has been reported by Watkins et al. (Watkins, 1995). High purity InAs epilayers were grown on GaAs substrates by MOCVD technique. Temperature dependent Hall measurements between 1.8 and 293 K showed a competition between bulk and surface conduction, with average Hall mobilities of $1.2 \cdot 10^5$ $cm^2/V \cdot s$ at 50 K. Large changes in the temperature dependent transport data are observed several hours after Hall contact formation and appear to be due to passivation of the surface accumulation layer by native oxide formation. The highest electron mobilities were observed in InAs films grown by MOCVD at reduced growth temperature (Partin, 1991). Electron mobilities as high as 21000 $cm^2/V \cdot s$ at 300 K were obtained for a film only 3.4 μm thick. From the depth dependence of transport properties it has been found that in the grown films electrons are accumulated near the air interface of the film, presumably by positive ions in the native oxide. The scattering from dislocations was greatly reduced in the surface accumulation layer due to screening by a high density of electrons. These dislocations arise from lattice mismatch and interface disorder at the film-substrate interface, preventing these films from obtaining mobility values of bulk indium arsenide. More or less successful attempts to grow quality InAs epitaxial films were also reported in numerous papers (Fukui, 1979; Haywood, 1990; Egan, 1995; Huang, 1995; von Eichel-Streiber, 1997; Watkins, 1997).

Technology of InSb bulk crystals is more mature than HgCdTe. Good quality substrates with more than 7 cm diameter are commercially available (Micklethwaite, 2000). However, technology of InSb and InAs epitaxial layers is not matured to the level suitable for device applications.

3.2. Junction formation techniques

3.2.1. HgCdTe photodiodes

Different HgCdTe photodiode structures have been developed including mesa, planar and lateral homojunction and heterojunction structures. The history and current status of HgCdTe IR photodiodes has been reviewed in numerous monographs and review articles (Capper and Elliot, 2001; Norton,1999; Rogalski, 2011; Rogalski et al., 2000; Chu and Sher, 2010; Reine, 2000; Baker and Maxey, 2001; Sher, 1991). The junctions have been formed by numerous techniques including impurity diffusion, ion implantation, growth of doped epitaxial layers from vapor or liquid phase. In the early stages of device technology Hg in- and out-diffusion has been used for the junction formation in HgCdTe bulk material. At present

http://dx.doi.org/10.5772/52930

time ion implantation is commonly used technique for formation n-on-p and p-on-n homo- and heterojunctions. The n^+-p homojunction can be formed by implantation of different ions into a vacancy doped p–type material, but B and Be are the most frequently used for this purpose. The doses of 10^{12}–10^{15} cm^{-2} and energies of 30–200 keV are used for the junction formation. First devices were fabricated on bulk p-HgCdTe single crystals with the hole concentration of the order of 10^{16} cm^{-3}. But in the early 1990s bulk crystals were replaced by LPE material. To-day, epitaxial films grown by LPE on CdZnTe lattice matched substrates are the best structural quality material, and they are successfully used in the homojunction technology. An ion implantation was also adapted to produce P^+-n heterojunctions (P means wider gap material). In both structures the lightly doped 'base' region with the doping concentration below 10^{16} cm^{-3} determines the dark current and photocurrent. Indium is most frequently used as a well-controlled dopant for n-type doping due to its high solubility and moderately high diffusion. Arsenic proved to be the most successful p-type dopant that are used for fabrication of stable junctions due to very low diffusivity. The important advantage of P+-n structure is that the thermal generation of carriers is effectively reduced in wider bandgap material.

The significant step in the development of HgCdTe photodiodes has been made by Arias with co-authors (Arias, 1993). They proposed the double-layer planar heterostructure (DLPH) photodiodes. The photodiodes were realized by incorporating a buried narrow-bandgap active layer in the DLPH configuration. The planar devices were formed using a $Hg_{1-y}Cd_yTe/Hg_{1-x}Cd_xTe$ (y>x) heterostructure grown by MBE on CdZnTe substrate. An important feature of the DLPH approach is a planar p-doped/n-doped device geometry that includes a wide-bandgap cap layer over a narrow-bandgap 'base' layer. The formation of planar photodiodes was achieved by selective implanting of arsenic through a ZnS mask followed by diffusing the arsenic (by annealing at high temperature) through the cap layer into the narrow gap base layer. After that the structures were annealed under Hg overpressure. The first high-temperature annealing was carried out to diffuse the arsenic into the base layer and to make the doped region p-type by substitution of arsenic atoms on the Te sub-lattice, while the second low-temperature one was carried out to annihilate Hg vacancies formed in the HgCdTe lattice during high-temperature process. In DLPH photodiodes significant reduction in tunneling current and surface generation-recombination current has been achieved. The architecture of mesa and planar heterostructure photodiodes are shown in Fig.1. The back-illuminated heterostructure photodiodes prepared from both LPE and MBE material grown on CdZnTe substrates have the highest performance achieved to-day (Arias, 1993; Bajaj, 2000; Rogalski, 2000).

The serious disadvantage of CdZnTe substrates is the thermal expansion coefficient mismatch with Si used for the read-out integrated circuit. To overcome this problem, growth of HgCdTe on alternate substrates such as sapphire, Si and GaAs has been developed. LPE, MBE and MOCVD techniques were used for this purpose. However, these alternate substrate materials suffer from a large lattice mismatch with HgCdTe, leading to a higher defect density in the HgCdTe material and consequently reducing the detector performance (Bajaj, 2000). Despite these disadvantages the large, 1024-1024 and 2048-2048, HgCdTe FPAs operating in

SWIR and MWIR spectral bands were grown on alternative substrates (Kozlowski, 1999; Bajaj, 2000; Golding, 2003; Tribolet, 2003). Their performance is comparable to performance of FPAs prepared on lattice matched bulk substrates, with the same spectral cut-off.

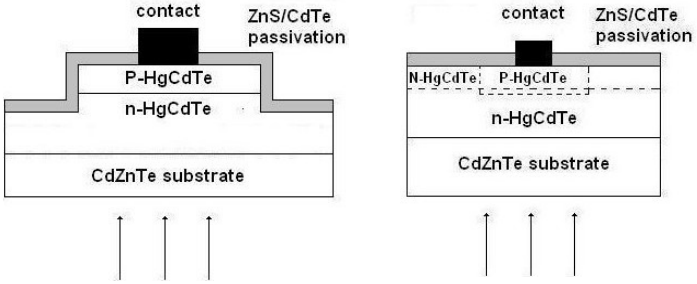

Figure 1. Schematic cross section of mesa (left) and planar (right) HgCdTe IR photodiodes. The photodiodes are illuminated through the wide bandgap substrate.

While ion implantation of As requires activation of the implanted atoms at relatively high temperatures, an alternative technology (ion milling or plasma induced type conversion) has received considerable attention during the past few years. Currently plasma induced type conversion in HgCdTe is regarded as an alternative to ion implantation junction formation technology (Agnihotri, 2002). The post-implant annealing is not needed in this technology. Reactive ion etching (RIE) induced type conversion and junction formation have been observed in a vacancy doped p-HgCdTe using H_2/CH_4 plasma. The junction depth could be adjusted from 2 to 20 μm.

3.2.2. InSb and InAs photodiodes

High performance InSb detectors have been fabricated with bulk material for decades. Typically, the p-on-n junctions are prepared on bulk crystals of n-type conductivity with electron concentration in the range 10^{14} - 10^{15} cm^{-3} and mobility of the order of (2-6) 10^5 cm^2 V^{-1} s^{-1} at T = 77 K. Be ion implantation and thermal diffusion of Zn and Cd seems to be the most frequently used technological methods which allow to obtain sharp p^+-n junctions (Mozzi and Lavine, 1970; Hurwitz and Donnelly, 1975; Rosbeck, 1981; Nishitani, 1983; Fujisada, 1985). The current status of InSb photodiode technology have presented by Wimmers et al. (Wimmers, 1983; Wimmers, 1988). Current manufacturing device processes require that bulk materials should be thinned before or after the junction preparation. Using this technique, hybrid FPAs were produced (Fowler, 1996; Hoffman, 1991; Parrish 1991). An array size of 1024-1024 was possible because the InSb detector material was thinned to <10 μm (after surface passivation and hybridization to a readout chip) which allows it to accommodate the InSb/silicon thermal mismatch. Certainly, the substrate thinning process is a very delicate process that can lower the yield and the reproducibility of the photodiodes, but it is used commercially because of LPE of InSb is not developed. Several attempts have been made to manufacture InSb photodiodes by LPE (Kosogov and Perevyaskin, 1970; Kazaki, 1976).

http://dx.doi.org/10.5772/52930

Currently the major efforts are focused on photodiodes grown by MBE and MOCVD methods. An overview *of* these technologies has been done by Razeghi (Razeghi, 2003). The InSb photodiodes were grown on 3-inch Si and (111)GaAs substrates. The InSb photodiodes typically consisted of a 2 μm n^+ region (~10^{18} cm^{-3} at 77 K), a ~6 μm unintentionally doped region (n = 10^{15} cm^{-3} at 77 K) and a ~0.5 μm p^+ (~10^{18} cm^{-3}) contact layer. The crystallinity of these structure was excellent as confirmed by the X-ray diffraction, which showed FWHM <100 arcs for structures grown on (111)GaAs and Si substrates. Photodiodes were fabricated with 400 × 400 μm^2 mesa structures by photolithography and wet chemical etching. These devices showed excellent response of about 1000 V/W, which is comparable to that of bulk detectors, with detectivities of ~3 10^{10} $cmHz^{1/2}/W$ at 77 K. It was shown that photodiodes can operate up to room temperature, even though they were not optimized for this purpose.

A miniaturized InSb photovoltaic infrared sensor that operates at room temperature was developed by Kuze with co-authors (Kuze, 2007). The InSb sensor consists of an InSb p^+-p^--n^+ structure grown on semi-insulating GaAs (100) substrate, with a p^+-$Al_xIn_{1-x}Sb$ barrier layer between p^+ and p^-layers to reduce diffusion of photoexcited electrons. The optimum Al composition and thickness of AlInSb barrier layer was found to be x=0.17 and 20 nm, respectively. Typical responsivity of 1.9kV/W, output noise of 0.15 $\mu V/Hz^{1/2}$ and detectivity of 2.8 10^8 cm $Hz^{1/2}/W$ was measured at 300K. InSb high-speed photodetectors were grown on semi-insulating GaAs substrate with 0.1 μm GaSb buffer layer using MBE (Kimukin, 2003). After the buffer layer a 1.5 μm thick n-InSb layer, 1.5 μm thick n-InSb layer, and finally 0.5 μm thick p- InSb layer were grown. The n-active layer was unintentionally doped to 2-3 10^{15} cm^{-3}. Tellurium and beryllium were used as the n- and p-layer dopants, respectively. Doping level was 10^{18} cm^{-3} for both highly doped layers to decrease the serial resistance. The developed photodetectors can operate at room temperature. The responsivity 1.3 A/W was measured at 1.55 μm wavelength at room temperature. InSb photodiodes grown by MBE on GaAs coated Si substrates have been reported (Besikci, 2000; Ozer and Besikci, 2003). The peak detectivity of ~$1 \cdot 10^{10}$ cm $Hz^{1/2}$ W^{-1} at 80 K has been measured under backside illumination without anti-reflection coating. Differential resistance at 80 K is shown to be limited by ohmic leakage under small reverse bias and trap assisted tunneling under moderately large reverse bias.

InAs photodiodes are mainly manufactured by ion implantation and diffusion methods (McNally, 1970; Astahov, 1992). The p-n junctions prepared by Cd diffusion into n-InAs single crystals were investigated by Tetyorkin et al. (Tetyorkin, 2011). The photodiodes grown by MBE on InAs substrates have been reported (Kuan, 1996; Lin, 1997). The fabrication of InAs photodiodes on GaAs and GaAs-coated Si substrates by MBE have also been reported (Dobbelaere, 1992).

In conclusion, during the past ten years the impressive progress has been made in the growth of narrow-gap semiconductors by MBE, MOVPE and MOCVD on silicon, GaAs and sapphire substrates. It is expected that in the near future HgCdTe and InSb IR photodiodes will be grown directly on silicon for the low cost detectors with bi-spectral and multispectral capability.

3.3. Thermal annealing

In HgCdTe photodiodes prepared on bulk crystals and LPE films the active absorption region should be p-type with the hole concentration of the order of 10^{16} cm^{-3}. Because of the as-grown materials are strongly p-type with vacancy concentration $p>10^{17}$ cm^{-3}, they should be annealed. Due to importance of annealing, it has been intensively studied in HgCdTe (Capper, 1994; Capper, 1997; Capper 2011). The most important parameters of annealing are temperature, Hg vapor pressure and annealing duration. In HgCdTe (x = 0.2) Vydyanath determined the free hole concentration at 77 K as a function of the Hg partial pressure, P_{Hg}, at anneal temperatures between 140 and 655 ^{0}C. The concentration of doubly-ionized vacancies [V_{Hg}] is given by (Vydyanath, 1991):

$$[V_{Hg}]P_{Hg}= 1.7E28 \exp(-1.67 \text{ eV/kT})cm^{-3}atm$$

The hole concentration at 77 K is assumed to be equal to the concentration of vacancies. It was proved that there is no essential difference in the annealing behavior of bulk crystals and LPE epilayers. As seen, the same vacancy concentration can be obtained by combination of temperature and Hg vapor pressure. Obviously, samples annealed at lower temperature and pressure conditions would also have the lower concentration of interstitials and potentially the higher minority carrier lifetime. However, to reduce density of Te precipitates and dislocations high-temperature annealing should be performed (Capper, 2011). In epilayers grown on lattice-matched substrates (CdTe, CdZnTe) the dislocation density is in low-10^4 to mid-10^5 cm^{-2}. At the same time, in epilayers grown on alternative substrates the dislocation density exceeds 10^6 cm^{-2}. In LWIR epilayers grown by MBE on (211) GaAs and Si substrates the dislocation densities as low as 2.3 10^5 cm^{-2} have been obtained using high-temperature cycling between 300 and 490 °C (Shin, 1992). It has been shown that epilayers grown by MOCVD require a higher thermal annealing temperature than MBE material and the difference in dislocation reduction between MBE and MOCVD HgCdTe materials is caused by dislocation movement under high-temperature and thermal stress conditions. A strong correlation between minority carrier lifetime and dislocation density was observed. The effect of temperature cycling on the dislocation density was also investigated by Farrell et al. (Farrell, 2011). In-situ and ex-situ thermal cycle annealing methods have been used to decrease dislocation density in CdTe and HgCdTe. During the MBE growth of the CdTe buffer layer, the growth was interrupted and the layer was subjected to an annealing cycle within the growth chamber under tellurium overpressure. During the annealing cycle the temperature is raised to beyond the growth temperature (290 → 550 °C) and then allowed to cool before resuming growth again. This process was repeated several times during the growth. The in-situ thermal cycle annealing resulted in almost a two order of magnitude reduction in the dislocation density. The decrease of dislocation density was attributed to the movement of the dislocations during the annealing cycles and their subsequent interaction and annihilation. To decrease the dislocation density in HgCdTe layers grown on CdTe/Si composite substrates, ex-situ annealing has been performed in a sealed quartz ampoule under a mercury overpressure. It was found that the primary parameters that affect dislocation density reduction are the annealing temperature and the number of annealing cycles.

http://dx.doi.org/10.5772/52930

At last, high temperature anneal in Hg vapor is used to activate the dopant by substituting arsenic atoms on the Te sublattice. A lower temperature anneal (200–250 ^{0}C), performed immediately after the high temperature anneal, annihilates the Hg vacancies formed in the HgCdTe lattice during high temperature treatment.

Bulk, LPE, MOCVD and MBE grown high purity material subjected to low-temperature (<300 ^{0}C) Hg reach annealing are converted to n-type with the electron concentration which depends on the doping level of residual donors. In HgCdTe material for LWIR photodiodes the minimum electron concentration that can be obtained is ~(2-10) 10^{14} cm^{-3} and the mobility is ~6 10^4 cm^2/V s (Chu and Sher, 2008).

Techniques for improving the control of the Hg vacancy concentration was also reported by Yang et al. (1985), who deduced experimentally a relationship between the concentration of Hg vacancies, the annealing temperature, and the temperature of a Hg source. They also derived theoretically an analytic expression for this relationship. The annealing for MBE grown material can be conducted in-situ under ultra-vacuum conditions. In-situ annealing is very useful for production purposes. The improved ex-situ and in-situ annealing processes were developed for MOCVD grown films (Madejczyk, 2005).

The performance of LWIR photodiodes can be improved by post-implant annealing (Bubulac, 1998). The dramatic decrease of the dark current in LWIR photodiodes was observed due to low temperature annealing at 120-150 °C (Ajisawa and Oda, 1995). The improvements was explained by changes in both carrier concentration profile and p-n junction position determined by interaction of interstitial Hg atoms with vacancies in the vicinity of the junction during the annealing process.

Very scarce data are available in the literature concerning the annealing of InSb and InAs, both materials and devices. The effect of rapid thermal annealing and sulfur passivation on the quality of reactively sputtered SiO_2 on InAs were investigated. Results show that both rapid thermal processing and sulfur passivation cause a reduction in leakage current and oxide fixed charges. Annealing at temperature higher than 400 ^{0}C caused degradation. Also, passivation started to loose its effectiveness when structures are annealed at 500 °C (Eftekhari, 1997).

4. Carrier transport and recombination mechanisms

4.1. Tunnelling current in HgCdTe, InAs and InSb photodiodes

Tunneling current was observed by many authors in IR photodiodes made of narrow-gap A_2B_6 and A_3B_5 semiconductors (Rogalski, 1995). However, its nature seems to be understood in rare cases. For instance, the trap-assisted tunneling (TAT) via single level in the gap introduced by point defects was proved to be the main reason for the excess current in HgCdTe IR photodides at rather small reverse biases followed by the direct band-to-band (BTB) tunneling current at higher biases (Nemirovsky, 1992; Rosenfeld, 1992; He, 1996). In these photodiodes the trap-assisted tunneling current is shown to be a source of

the low-frequency 1/f noise. Similar results were also obtained in HgCdTe MIS structures (He, 1996). Dislocations are also known for a long time as a source of an excess current in semiconductor devices, especially when they intersect the depletion region of the p-n junction (Matare, 1971; Holt, 2007; Shikin, 1996; Whelan, 1969). As to InAs and InSb photodiodes the role of dislocations is not established clearly. Therefore, identification of the type of defects participating in the carrier transport in InAs and InSb IR photodiodes is a key problem for improvement of their performance. Usually TAT and BTB tunneling currents were analyzed in the reverse biased IR photodiodes. This analysis performed for the forward biased InAs and InSb photodiodes revealed new aspects of tunneling transport of carriers.

4.2. Dislocation-assisted tunnelling current in the forward-biased InAs and InSb photodiodes

The photodiodes were prepared on single-crystal substrates of n-type conductivity. In order to investigate effect of dislocations on the dark current, the substrates were cut from different parts of ingots grown by Bridgman technique. The density of dislocations in InAs substrates measured by the etch-pit method was of the order of 10^4 cm^{-2}. The damaged surface layers were removed using dynamic chemical-mechanical polishing in solution of methanol with 2% of Br_2. The electron concentration and mobility in the initial substrates were (2-3) 10^{16} cm^{-3} and (2-2.5) 10^4 $cm^2/V{\cdot}s$, respectively. The dislocation density was ranged from (1-2) 10^4 cm^{-2} in the central part of ingots up to 4 $\bullet 10^5$ cm^{-2} at the periphery one. The p-n junctions were prepared by thermal diffusion of preliminary synthesized $CdAs_2$ into substrates in sealed evacuated quartz ampules. The mesa structures with active area A = 7 10^{-3} cm^2 were delineated using standard photolithographic technique. Then Zn and In contact pads were thermally deposited onto p- and n-type sides of the junction, respectively, followed by a heat treatment in purified hydrogen atmosphere. InSb photodiodes were manufactured by implantation of beryllium into appropriately prepared substrates followed by thermal annealing. In n-InSb substrates the electron concentration and mobility were of the order of (1-2) 10^{15} cm^{-3} (6-7) 105 $cm^2/V{\cdot}s$ at 77 K, respectively. The dislocation density in InSb substrates was not exceeded 5·102 cm-2. Photodiodes had planar structure with the junction area A = 1.33 10^{-2} cm^2.

The current-voltage characteristics are shown in Fig.2. As seen, the characteristics consist of two exponential parts. At lower bias voltages the forward current in InAs photodiodes increases with increasing the density of dislocations, whereas at higher voltages it has approximately the same magnitude for both photodiodes. Fig. 3 shows the temperature dependence of the forward current in InAs and InSb photodiodes measured at the bias voltage 10 mV. At low temperatures $T < 130$ K the current is weakly dependent on temperature. At the same time at higher temperatures it exhibits an activation character. To clarify the observed peculiarities the current-voltage characteristics were investigated in InAs photodiode subjected to ultrasonic treatment with frequency 5-7 MHz and intensity ~0.4 W/cm^2 during four hours at room temperature, Fig. 4.

http://dx.doi.org/10.5772/52930

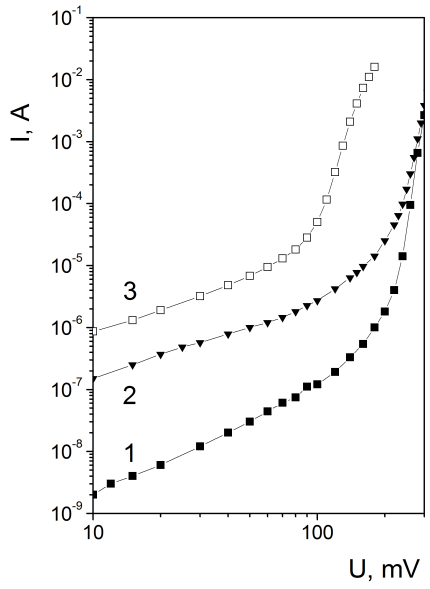

Figure 2. Current-voltage characteristics in InAs (1,2) and InSb (3) photodiodes at 77 K. Curves (1) and (2) refer to the dislocation density in substrates 4 10^4 cm^{-2} (1) and 2 10^5 cm^{-2}, respectively.

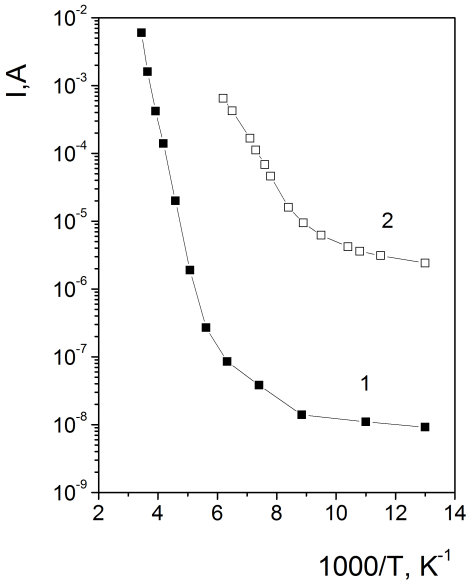

Figure 3. Temperature dependences of the forward current measured at 10 mV in InAs (1) and InSb (2) photodiodes

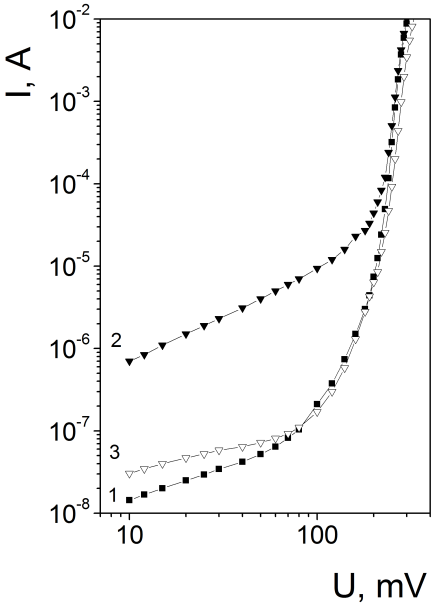

Figure 4. Current-voltage characteristics in InAs photodiodes before and after ultrasonic treatment (curves 1 and 2, respectively), and after one-year storage (3).

The dark current as a function of bias voltage was measured immediately after ultrasonic treatment as well as after approximately one-year storage of photodiodes at laboratory condition. It must be pointed out that the ultrasonic treatment results in pronounced increase of the dark current at lower bias voltages, whereas those parts of the current-voltage characteristics measured at higher voltages were remained almost unchanged. Also, it is important to note that after storage of samples within one year the excess current caused by ultrasonic treatment is decreased to approximately the starting values.

An explanation of experimental results is based on the assumption that dislocations intersecting the depletion region are responsible for the excess current at small forward biases. A model for tunneling current via dislocations intersecting the depletion region of the junction has been proposed by Evstropov et al. (Evstropov, 1997, 2000). Experimentally it has been also investigated by Ageev with co-authors (Ageev, 2009). According to this model, mobile carriers (holes and electrons) are moved along acceptor-like and donor-like dislocation lines which has been modeled by a chain of parabolic potential barriers with variable height.

In the symmetric junction the forward current flows due to direct recombination of electrons and holes at the middle of the depletion region. The current-voltage characteristics can be described by the formula

http://dx.doi.org/10.5772/52930

$$I = I_{01}\exp\left(\frac{e(U - IR_s)}{E_0}\right) + I_{02}\exp\left(\frac{e(U - IR_s)}{\beta kT}\right) \quad (1)$$

where I_{01} and I_{02} are the pre-exponential factors, E_0 is the characteristic energy; β is the ideality factor and R_S is the series resistance.

The temperature dependence of the pre-exponential factor in equation (1) is then given by:

$$I_{01} = e\rho\nu_D A\exp\left(\frac{eU_D}{E_0}\right) \quad (2)$$

where ϱ is the density of dislocations, ν_D is the Debye frequency, U_D is the diffusion potential. The lifetime of carriers in the depletion region $\tau 0$ was determined from the relation $I_{02} = en_iWA/\tau_0$, where n_i is the intrinsic concentration of carriers, W is the depletion region width, A is the junction area.

Because of in the investigated photodiodes the diffusion potential linearly depends on temperature (Sukach, 2005), the exponential dependence of I_{01} on temperature should be observed. Also, in accordance with Evstropov, the characteristic energy E0 is independent on the concentration of free carriers. These consequences of the analyzed model may be used for discrimination of the tunneling current via dislocations. For instance, by using typical experimental data for InSb photodiodes at 77 K ($I_0/A = 8.85\bullet10^{-5}$A/sm^2, U_D = 160 mV, E_0 = 29 meV and $\nu_D = 3.3\bullet10^{12}$ s^{-1}, which was determined from the known value of Debye temperature T_D = 160 K (Madelung, 1996), the dislocation density ϱ = $4.2\bullet10^4$ cm^{-2} was estimated. This value is almost two orders of magnitude higher than in the starting substrates. Relatively high density of dislocations can be explained by the fact that during the heat treatment the edge of the junction was not removed from the zone of radiation defects formed by ion implantation of beryllium in InSb. However, the same discrepancy between experimental and theoretical data was also observed in InAs photodiodes prepared by diffusion technique. Moreover, in the investigated InAs photodiodes the characteristic energy E_0 was found to be varied from ~30 meV up to ~60 meV in contrast to theoretical predictions. It must be stressed that values of E_0 experimentally obtained in this study are close to those observed in diodes made of wide-gap GaP and SiC (Evstropov, 1997, 2000; Ageev, 2009). This means that the tunneling current via dislocations is characterized by the same features independent on semiconductor materials used for manufacture of diode structures.

The observed discrepancy between theoretical and experimental data may be caused by several reasons. First of all, in the model developed by Evstropov dislocation lines are assumed to be fully occupied by carriers and have a length of the order of the depletion region width. This seems to be not typical for dislocations in semiconductors (Matare, 1971; Holt and Yacobi, 2007; Shikin, 1995). Also, the presence of jogs, inclusions of impurity atoms, kinks, etc., results in a loss of translation symmetry along the dislocation line and spatial localization of mobile carriers. Thus only short dislocation segments can contribute to the direct current conduction (Holt, 2007; Kveder, 1985; Nitcki, 1985). It is supposed that this is the main reason why the direct current conduction along dislocation cores is not clearly demonstrated so

far (Holt and Yacobi, 2007). Further, as originally proposed by Shockley (Holt and Yacobi, 2007) and according to Labusch (Labusch, 1982) and Labusch and Schröter (Labusch and Schröter, 1983) dislocations in semiconductors introduce one-dimensional energy bands into the gap, located near the conduction and valence band edges. Direct recombination transitions between these bands seem to be not effective. The much more effective is the recombination through deep defect states in the gap (Kveder, 2001; Seibt, 2009).

Further analysis of experimental data is based on assumption that the p-n junctions in the investigated diodes are non-homogeneous and there are two conduction paths for mobile carriers in the junction. The tunneling current flows via the dislocations intersecting the depletion region whereas the recombination current flows via homogeneous region free of dislocations. At low bias voltages the tunneling current is dominant, so the forward I-U characteristic is described by the first term in equation (1). Thus, the weak dependence of the forward current on temperature in Fig.3 can be qualitatively understood. With increasing the bias voltage this current is masked by the recombination current which can be explained within the well known SRH model (Sze, 1981). This change in the current mechanism is described by the second term in equation (1).

Experimental evidences exist that the recombination rate of minority carriers at dislocations in silicon depends strongly on dislocation decoration by transition metal impurities (Seibt, 2009). Due to the fact that the recombination of carriers captured at dislocation bands can be substantially enhanced by the presence of small amount of impurity atoms at the dislocation core, it is assumed that the low-temperature transport mechanism consists of several steps, namely: a) injection of electrons into the depletion region under the forward bias, b) capture of electrons on the dislocation core by tunneling transitions, c) electron transport along the undisturbed segments of the dislocation core and d) recombination of electrons with holes through the states in the gap related with 'native' core defects (such as jogs and kinks) or impurity atoms segregated to the dislocation core. In the case of the dislocation core can exchange electrons directly with the conduction band the energy E_0 is the dislocation barrier height. Using experimental values for the density of dislocations (~10^4 cm^{-2}) and the forward current (10^{-8}-10^{-7} A) it is easy to show that dislocations form equipotential lines. If we take into account that the dislocation resistivity is of the order of 10^{10} Ω/cm (Labusch, 1982), the voltage drop along a segment of dislocation of 10^{-5} cm is less than 10^{-4} V. So, it is likely that at low temperatures tunneling transitions of electrons to the dislocation core is the bottleneck for the forward current in the investigated photodiodes. Also, it is possible that these transitions can occur via local states in the gap, associated with point defects or their precipitates surrounding dislocations. In this two-step process physical meaning of E_0 should be corrected taking into account the energy of these states. Because of in this study the prethreshold intensity of ultrasonic treatment was used, experimental results can be explained by rearrangement of existing defects rather than generation of new point defects. In accordance with the vibrating string model of Granato-Luecke, the intensive sonic-dislocation interaction results in an effective transformation of the absorbed ultrasonic energy into the internal vibration states of a semiconductor stimulating different defect reactions (Granato

http://dx.doi.org/10.5772/52930

and Luecke, 1956). The driving force of the long-term relaxation of the forward current may by stress and electric fields around dislocations.

In conclusion, the excess current experimentally observed in InAs and InSb photodiodes at forward biases is related to dislocations intersecting the depletion region. Pronounced effect of ultrasonic treatment on the forward current is explained by transformation of defects segregated around dislocations. A model for the carrier transport via dislocations is proposed.

4.3. Trap-assisted tunnelling current in the reverse-biased InAs and InSb photodiodes

The effect of traps in the depletion region of a photodiode on the TAT current was considered by several authors (Wang, 1980; Kinch, 1981; Nemirovsky, 1989, 1991; Rosenfeld and Bahir, 1992; He and Celik-Butler, 1995). The calculation of the TAT current in a reverse-biased photodiode is carried out using several simplifying assumptions: the p-n junction is abrupt with a linear variation of potential (constant electric field) across the depletion region; the traps are uniformly distributed; the initial states are occupied whereas the final states are empty. Under these assumptions, the TAT current is proportional to the trap density, but depends exponentially on the trap-ionization energy and the electric field strength. Within this model the observed soft reverse breakdown current-voltage characteristics were adequately explained.

For instance, in Fig. 5 and 6 are shown typical current-voltage characteristics and 1/f noise spectra measured in n^+-p HgCdTe (x=0.22) photodiodes. The photodiodes were prepared by boron implanting into epitaxial films grown by LPE method, followed by surface passivation and low-temperature post-implanting anneal. In the calculation of TAT current thermal and tunnel transitions from the valence band to deep defect states in the gap followed by tunnel transitions to the conduction band were taken into account. That is, the TAT current is given by

$$J_{tat} = qWN_t\left(\frac{1}{\omega_v N_v + c_p p_1} + \frac{1}{\omega_c N_c + c_n n_1}\right)^{-1} \tag{3}$$

were $\omega_c N_c$ and $\omega_v N_v$ are the tunneling rates. In order to fit experimental and calculated data it has been supposed that are non-uniformly distributed through the depletion region (Ivasiv, 1999). The best fit was obtained for the acceptor-like traps with energy $E_t = 0.72E_g$ above the top of the valence band and the capture rates for holes and electrons $C_p \approx 10^{-7}$ - 10^{-6} cm^3/s and $C_n = (0.1\text{-}0.01)C_p$, respectively. The determined trap energy correlates well with the previously used $E_t=0.75E_g$ in photodiodes prepared by boron implantation to bulk material (Nemirovsky, 1991). Note that in photodiodes investigated by Nemirovsky et al., the TAT current was dominant by donor-like traps with the capture rates $C_p=(10^{-10}\text{-}10^{-9}cm^3/s)$ and $C_n = (10\text{-}100)C_p$. Our data are in accordance with the study performed by Rosenfeld and Bahir for acceptor-like centers in HgCdTe photodiodes (Rosenfeld and Bahir, 1992).

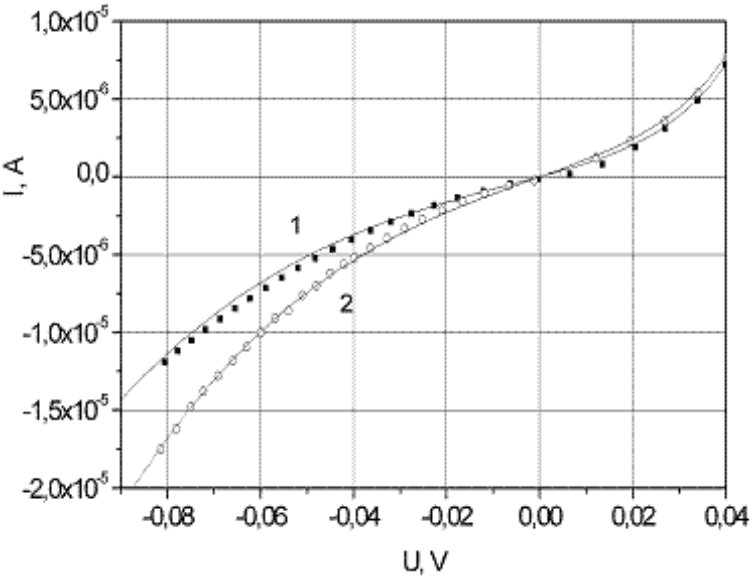

Figure 5. Measured (dots) and calculated (solid lines) current-voltage characteristics of n^+-p photodiodes at 77 K. Parameters of traps: E_t=0.72E_g, C_p=1 10^{-7} cm^3/s, C_n=0.01C_p. N_t=3.2 10^{15} and 4.8 10^{15} cm^{-3} for curves 1 and 2, respectively.

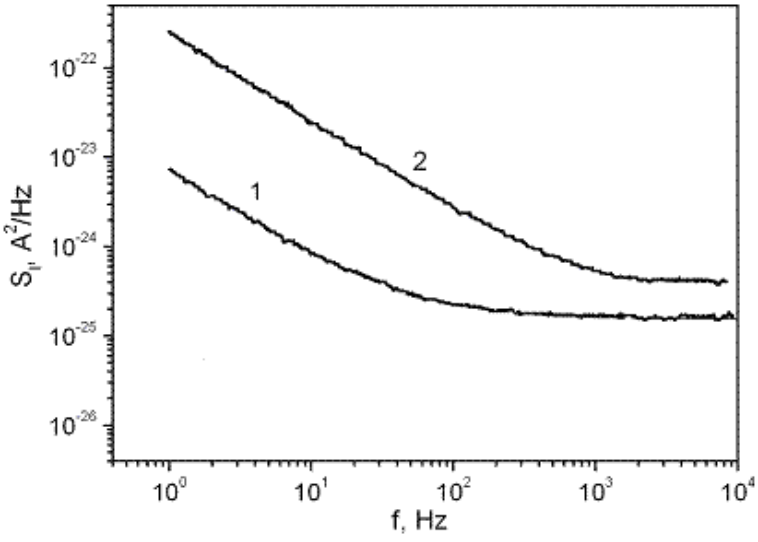

Figure 6. Noise spectra for the photodiodes with R_0A=1.0 Ω cm^2 (1) and R_0A=0.3 Ω cm^2 (2) at 77 K.

http://dx.doi.org/10.5772/52930

The correlation was found between the TAT current at small reverse bias voltage U ≤ 0.1 V and 1/f noise. In the case of the total dark current was completely determined by TAT mechanism the 1/f noise was observed up to frequencies 10^4 Hz. Taking this into account the noise current was calculated by the formula

$$I_n = \alpha \left(\frac{I_{TAT}}{\sqrt{f}} \right) \tag{4}$$

From the fitting calculation the values of the constant $\alpha = 10^{-8}$ - 10^{-7} were found. Earlier similar correlation was observed by Nemirovsky et al.. (Nemirovsky, 1989; Nemirovsky, 1992).

It seems that parameters of traps determined from the fitting calculations within this model may be used for rough estimations only. More accurate calculations of the TAT current has been performed by Krishnamurthy et al. (Krishnamurthy, 2006). The TAT current has been calculated for a linearly varying electric field in the depletion region of the p-n junction and self consistently obtained trap-occupation probability. The calculations showed that the reverse-bias dark current changes considerably both in magnitude and in shape. For a better interpretation of the observed dark currents and an estimation of trap density, these improvements should be taken into account.

In order to explain experimental data in InAs photodiodes it has been assumed that the tunneling current is controlled by small areas of the junction which are characterized by large deviation of impurity concentration from the mean value (Sukach, 2005). For instance, non-uniform distribution of impurity atoms can be realized around dislocations (Cottrell atmosphere) or at the periphery of the junction. This results in increase of electric field in the junction over the value given by the equation (1) for more or less uniform distribution of charged defects in the junction. We also assumed that the tunneling current in these areas is caused by the trap-assisted tunneling described with the modified values of the junction area and electric field strength in the junction. For this purpose, the dislocation was modeled by the effective area $A_{eff} \approx 1$ μm^2 with increased concentration of charged defects. Their concentration was determined from the fitting calculation of I-U curves. The density of dislocation was assumed to be of the order of 10^4 cm^{-2}. The electric field around a dislocation may be determined from the Poisson equation. However, as the first approximation there has been assumed that the electric field around dislocations may be estimated using formulas for the abrupt p-n junction (Sze, 1981). Because of the tunneling rates $\omega_c N_c$ and $\omega_v N_v$ are exponentially depend on the electric field strength, the TAT current through these regions are exponentially large in comparison with the uniform regions of the junction. The trap-assisted tunneling current was calculated for the following cases: i) traps are exchanged with both bands by thermal and tunnel transitions of carriers (curve 1), ii) tunnel transitions of carriers from the valence band to traps followed by thermal and tunnel transitions to the conduction band (curve 2), tunnel transitions of carriers from the valence band to the conduction band through traps. The best fit was obtained for the energy of traps $E_t = E_g/2$ and their concentration in the range from ~10^{13} to ~10^{14} cm^{-3}. These values seem to be reasonable for InAs. The concentration of charged defects determined from the fit of the calculated and measured da-

ta was found to exceed $4 \cdot 10^{16}$ cm^{-3}. This value is more than one order of magnitude higher than the mean value of the free carriers concentration determined from the capacitance-voltage measurements.

Some arguments in favor of the measured current in InAs photodiodes is related to Cottrell's atmospheres around dislocations have been obtained from investigations of effect of ultrasonic treatment on the current-voltage characteristics (Sukach and Tetyorkin, 2009). In the photodiodes subjected to ultrasonic vibration with frequency 5-7 MHz and pre-threshold intensity ~0.4 W/cm^2 prononced increase of the reverse current was obseved. The current is relaxed down to the starting value during nine-month storage of photodiodes at laboratory conditions. Experimental results are explained by transformation of existing complex defects rather than generation of new point defects. Most probably that this transformation is connected with Cottrell's atmospheres around dislocations which intersect the p-n junction. In accordance with the vibrating string model of Granato-Luecke (Granato and Luecke, 1966), the intensive sonic-dislocation interaction results in an effective transformation of the absorbed ultrasonic energy into the internal vibration states of a semiconductor stimulating different defect reactions. The driving force of the observed relaxation may be deformation and electric fields around dislocations.

4.4. Recombination mechanisms

The carrier lifetime in HgCdTe, InSb and InAs narrow-gap semiconductors is determined by three principal recombination mechanisms: radiative, Auger and SRH. The first two mechanisms are intrinsic, whereas SRH recombination is not intrinsic because it is carried out with assistant of deep defect states in the gap. In principle, SRH recombination can be suppressed by reducing the concentration of recombination centers. Ten types of possible band-to-band Auger recombination processes in n- and p-type semiconductors were determined by Beattie (1962). The Auger 1 recombination mechanism in n-type material with InSb-like parabolic band structure was firstly considered by Beattie and Landsberg (Beattie and Landsberg, 1959). The Auger 7 process is important in p-type material (Beattie and Smith, 1967; Petersen,1970; Takeshima, 1972; Casselman and Petersen, 1980; Casselman, 1981). For the nonparabolic band structure, the $|F_1F_2|$ dependence on k, and nongenerate statistics appropriate expressions for the Auger 7 recombination process has been deduced by Beattie and Smith (1967).

The well known problem in the Auger recombination processes is the uncertainty in the carrier lifetime introduced by the overlap integrals F_1 and F_2 of the periodic part of the electron wave functions. As was shown by Petersen (1970, 1981), the dependence of the product $|F_1F_2|$ on the wave vector k should be taken into account in p-type materials. However, in practice the constant value of $|F_1F_2|$ in the range 0.1-0.3 is used for calculations of the carrier lifetime (Rogalski, 1995). This results in scatter of the calculated data within an order of magnitude. The detailed analysis of recombination process in HgCdTe can be found in numerous review articles and books (Beattie and Landsberg, (1959); Petersen, 1981; Capper, 1994; Rogalski, 2011; Chu and Sher, 2010).

http://dx.doi.org/10.5772/52930

Due to Capper (1994), in n-type HgCdTe for low values of composition (x<0.25) and carrier concentrations >10^{15} cm^{-3} the Auger 1 recombination process is dominant, particularly at high temperatures (>100 K). The SRH recombination is important at lower values of carrier concentration and at low temperatures. In LPE material grown from Hg-rich solution higher values of lifetime than in corresponding material grown by other techniques were observed, presumably due to a lower level of recombination centers related with Hg vacancies. Dislocations can also contribute to the SRH recombination when present at high densities. The measured data in p-type HgCdTe indicated that the Auger 7 recombination does not limit the carrier lifetime. It is believed that the SRH recombination can explain most of the experimental data (Fastow, 1990).

The Auger recombination process in narrow-gap semiconductors with the three- and four-band Kane models of band structure was reexamined by Gelmomnt et al. (Gelmont, 1978; Gelmont, 1981; Gelmont, 1982; Gelmont and Sokolova, 1982). The appropriate calculations of the carrier lifetime in InAs based on Gelmont's theory has been performed by Tetyorkin and co-authors (Tetyorkin, 2011). The calculated dependences of the lifetime as a function of the carrier concentration in InSb is shown in Fig. 7 and 8.

The generation rate for the Auger 1 process g_{A1} obtained by Beattie and Landsberg is given by

$$g_{A1} = \frac{8(2\pi)^{5/2} e^4 m_e^* |F_1 F_2|^2 n_o}{h^3 \varepsilon^2 (1+\mu)^{1/2}(1+2\mu)} \left(\frac{kT}{E_g}\right)^{3/2} \exp\left[-\left(\frac{1+2\mu}{1+\mu}\right)\frac{E_g}{kT}\right] \tag{5}$$

According to Gelmont, the generation rate for the Auger 7 is

$$g_{A7}^{G} = \frac{18 m_o (m_{h\,h}^* / m_o) e^4}{\pi \hbar^3 \varepsilon^2} p_o \left(\frac{kT}{E_g}\right)^{7/2} \exp\left[-(1+\frac{m_{hl}^*}{m_{hh}^*})\frac{E_g}{kT}\right] g(\alpha) \tag{6}$$

In these equations, ε is the static dielectric constant, m_{hl}^* and m_{hh}^* are the effective masses of light and heavy holes, respectively, μ is the ratio of the electron to the heavy-hole effective mass. In the calculation of g_{A1} the product of the overlap integrals $|F_1F_2|$ is equal to 0.25 (Malyutenko, 1980). The calculated dependences are compared with experimental data published starting from the late 1950s to our days. As seen from Fig.7, the Auger 1 process is dominant at the electron concentration n > 4·10^{15} cm^{-3}, whereas at n < 1·$10^{15}$$cm^{-1}$ the carrier lifetime is determined by the radiative mechanism. In p-InSb the radiative recombination is dominant at the concentration p< 5·10^{15} cm^{-3}, Fig.8. The observed scatter of experimental data in samples with approximately the same concentration of carriers can be attributed to the SRH recombination. The values of the carrier lifetime in samples investigated earlier were lower than those obtained later. Thus, the relation between the improvement in technology of InSb and the increase in the carrier lifetime is clearly seen from experimental data shown in Fig. 7 and 8.

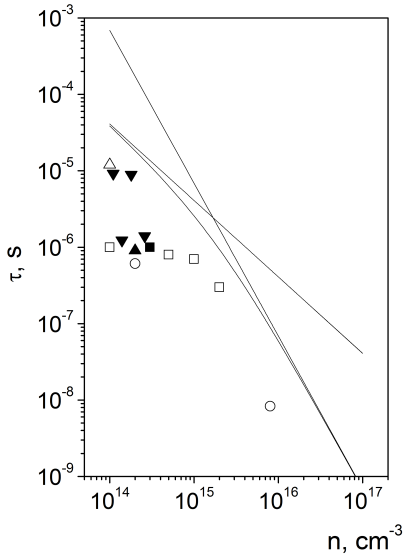

Figure 7. Calculated dependences (solid lines) of the lifetime in n-InSb at 77 K. Experimental are taken from (Abduvakhidov, 1968; Malyutenko, 1980; Guseinov, 1971; Strelnikova, 1993; Biryulin, 2004): open square, close square, open triangle, close triangle and open circle, respectively.

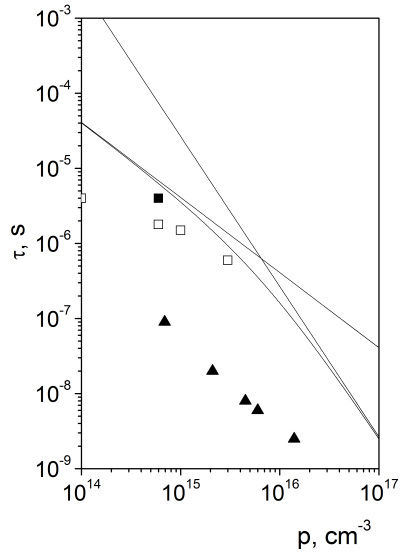

Figure 8. Calculated dependences (solid lines) of the lifetime in p-InSb at 77 K. Experimental data are taken from (Laff and Fan, 1961; Volkov, 1967; Zitter, 1959): close square, open square and close triangle, respectively.

http://dx.doi.org/10.5772/52930

In conclusion, the following peculiarities of the carrier lifetime in MWIR and LWIR HgCdTe may be pointed out: carrier lifetime can be essentially different in samples prepared by different growth techniques, even if they have approximately the same carrier concentration; correlation between the lifetime and the concentration of vacancies is observed in vacancy doped materials; lifetime can be increased by doping with foreign impurities; SRH recombination is more distinct at low temperatures and in samples with low carrier concentration.

It seems that the SRH recombination is also dominant in InAs and InSb at low temperatures and low values of the carrier concentration. It should be noted that the low-temperature annealing of n-InSb leads to a significant increase in the lifetime in samples with the carrier concentration of the order of 10^{14} cm^{-3}. The highest values of the lifetime, as shown in Fig.6 (Strelnikova, 1993), were obtained in annealed samples due to significant decrease in the concentration of recombination centers.

5. Conclusion

Despite significant advances in the development of infrared photodiodes on narrow-gap II-VI and III-V semiconductors, theoretically predicted threshold parameters have not yet been achieved. The main reason for this is the participation of defects of different type in the processes of recombination and carrier transport. It is clear that further progress in development of IR photodiodes is closely connected with the band gap and defect engineering. The most impressive application of these concepts, based on knowledge of fundamental physical properties and defect states in narrow-gap semiconductors, is the development of HgCdTe planar heterostructure photodiodes with the highest performance achieved to-day.

Author details

Volodymyr Tetyorkin[1], Andriy Sukach[1] and Andriy Tkachuk[2]

1 V. Lashkaryov Institute of Semiconductor Physics NAS of Ukraine, Ukraine

2 V. Vinnichenko State Pedagogical University, Ukraine

References

[1] Abaeva, T. V., Bublik, V. T., Morozov, A. N., & Pereverzev, A. T. (1987). Effect of In and Sb vacancies on temperature dependence of InSb lattice parameter at high temperatures, Izv. Akad. Nauk SSSR, Neorg. Mater. (In Russia), 0000-2337X., 23(2)

[2] Abduvakhidov, J. M., Volkov, A. S., & Golovanov, V. V. (1968). The study of the kinetics of photoconductivity and noise spectrum in InSb, Sov. Phys. Semicond., 0015-3222, 2(1)

[3] Adomaytis, E., Dorovolskis, Z., & Krotkus, A. (1984). Picosecond photoconductivity of indium arsenide, Sov. Phys. Semicond.,0015-3222, 18(8)

[4] Adrianov, D. G., Karataev, V. V., Lazarev, G. V., et al. (1977). On the interaction of carriers with localized magnetic moments in InSb: Mn, Sov. Phys. Semicond., 0015-3222, 11(7)

[5] Ageev, O. A., Belyaev, A. E., Boltovets, N. S., Ivanov, V. N., Konakova, R. V., Kudryk, Ya., Ya, , Lytvyn, P. M., Milenin, V. V., & Sachenko, A. V. (2009). Au-TiBx –n-6H-SiC Schottky barrier diodes: the features of current flow in rectifying and nonrectifying contacts, Semiconductors,0015-3222, 43(7)

[6] Agnihotri, O. P., Lee, H. C., & Yang, K. (2002). Plasma induced type conversion in mercury cadmium telluride, Semicond. Sci. Technol., R11-R19, 0268-1242, 17

[7] Ajisawa, A., & Oda, N. (1995). Improvement in HgCdTe Diode Characteristics by Low Temperature Post-Implantation Annealing, J. Electron. Mater., 0361-5235, 24(9)

[8] Allaberenov, O. A., Zotova, N. V., Nasledov, D. N., & Neuimina, L. D. (1970). Photoluminescence of n-InAs, Sov. Phys. Semicond.,0015-3222, 4(10)

[9] Arias, J. M. (1994). Growth of HgCdTe by molecular beam epitaxy, in Properties of Narrow Gap Cadmium-Based Compounds, Capper P. (ed.), INSPEC, London, 0-85296-880-9, 30-35.

[10] Arias, J. M., Pasko, J. G., Zandian, M., Kozlowski, L. J., & De Wames, R. E. (1994a). Molecular beam epitaxy HgCdTe infrared photovoltaic detectors, Opt. Eng., 0091-3286, 33

[11] Arias, M., De Wames, R. E., Shin, S. H., Pasko, J. G., Chen, M., & Gertner, E. R. (1989). Infrared diodes fabricated with HgCdTe grown by molecular beam epitaxy on GaAs substrates, Appl. Phys. Lett. 0003-6951, 54(11), 1025-1027.

[12] Arias, M., Pasko, J. G., Zandian, M., Shin, S. H., Williams, G. M., Bubulac, L. O., De Wames, R. E., & Tennant, W. E. (1993). Planar p-on-n HgCdTe heterostructure photovoltaic detectors, Appl. Phys. Lett., 0003-6951, 62(9)

[13] Astahov, V. P., Danilov, Yu. A., Dutkin, V. F., Lesnikov, V. P., Sidorova, G., Yu, , Suslov, L., A., , Taubkin, I. I., & Eskin, Yu. M. (1992). Planar photodiodes based on InAs material, Techn. Phys. Lett. (In Russia), 0320-0116, 18(3)

[14] Bagai, R. K., Selth, G. L., & Borle, W. N. (1983). Growth of high purity indium antimony crystals for infrared detectors, Indian J. Pure Appl. Phys., 0019-5596, 21

[15] Bajaj, J. (2000). State-of-the-art HgCdTe Infrared Devices, Proc. SPIE, 0027-7786X., 3948

[16] Baker, I. M., & Maxey, C. D. (2001). Summary of HgCdTe 2D array technology in the U.K., J. Electron. Mater. 0361-5235, 30(6)

[17] Balagurov, L. A., Omel'yanovskii, E. M., & Fistul', V. I. (1977). The energy position of deep levels in high-resistance InAs: Cr, Sov. Phys. Semicond.,0015-3222, 11(2)

[18] Balderschi, A., & Lipari, N. O. (1974). Cubic contribution to the spherical model of shallow acceptor states, Phys. Rev. B., 1050-2947, 9(4)

[19] Baranov, A. N., Voronina, T. I., Gorelenok, A. A., et al. (1992). Study of structural defects in epitaxial layers of indium arsenide, Semiconductors., 0015-3222, 26(9)

[20] Baranov, A. N., Voronina, T. I., Lagunova, T. S., et al. (1993). Properties of epitaxial indium arsenide doped with rare-earth elements, Semiconductors, 0015-3222, 27(3)

[21] Bazhenov, N. L., Zegrya, G. G., & Ivanov-Omskii, V. I. (1997). Electroluminescence in the separated heterostructure of p-GaInAsSb/p- InAs at liquid helium temperatures, Semiconductors, 0015-3222, 31(10)

[22] Beattie, A. R. (1962). Quantum Efficiency in InSb, J.Phys.Chem.Solids, 0022-3697, 23

[23] Beattie, A. R., & Landsberg, P. T. (1959). Auger effect in semiconductors, Proc. Roy. Soc. A., 0308-2105, 249

[24] Beattie, A. R., & Smith, G. (1967). Recombination in semiconductors by a light hole Auger transition, Phys. Stat. Solidi, 0031-8965, 19

[25] Benz, K. W., & Müller, G. (1979). GaSb and InSb crystals grown by vertical and horizontal travelling heater method. J. Crystal. Growth, 0022-0248, 46

[26] Berding, M., van Schilfgaarde, M., & Sher, A. (1994). First-principles calculation of native defect densities in Hg0.8Cd0.2Te, Phys. Rev. B., 0163-1829, 50(3), 1519-1534.

[27] Berding, M. A., Sher, A., & van Schilfgaarde, M. (1995). Defect modeling studies in HgCdTe and CdTe, J. Electron. Mat., 0361-5235, 24

[28] Berding, M. A. (2011). Defects in HgCdTe-Fundamental, in Mercury cadmium telluride : growth, properties, and applications, Capper, P. and Garland, J. (eds.), Wiley, 978-0-47069-706-1, 263-273.

[29] Besikci, C. (2000). III-V infrared detectors on Si substrates, Proc. SPIE, 0027-7786X, 3948

[30] Biryulin, P. V., Turin, V. I., & Yakimov, V. B. (2004). Investigation of the characteristics of InSb photodiode arrays, Sov. Phys. Semicond., 0015-3222, 38(4)

[31] Blaut-Blachev, A. N., Ivlev, V., & S.and, Selyanina. V. I. (1979). Fluoride-fast diffusing acceptors in indium antimonide, Sov. Phys. Semicond., 0015-3222, 13(11)

[32] Boieriu, P. C., Grein, H., Garland, J., et al. (2006). Effects of hydrogen on majority carrier transport and minority carrier lifetimes in long-wavelength infrared HgCdTe on Si, J. Electron. Mater., 0361-5235, 35(6)

[33] Bornfreund, R., Rosbeck, J. P., Thai, Y. N., Smith, E. P., Lofgreen, D. D., Vilela, M. F., Buell, A. A., Newton, M. D., Kosai, K., Johnson, S. M., De Lyon, T. J., Jensen, J. J., & Tidrow, M. Z. (2007). High-Performance LWIR MBE-Grown HgCdTe/Si Focal Plane Arrays, J. Electron. Mater., 0361-5235, 37

[34] Bublik, V. T., Blaut-Blachev, A. P., Karataev, V. V., Mil'vidskii, M. G., et al. (1977). Nature of intrinsic point defects in indium arsenide and their effect on electrophysical proiperties of single crystals, Kristalografiya (Sov. Phys. Crystallogr.), 0023-4761, 22(6)

[35] Bublik, V. T., Karataev, V. V., Mil'vidskii, M. G., et al. (1979). Defects in heavily doped with donor impurities of Group VI single crystals of indium arsenide, Kristalografiya (Sov. Phys. Crystallogr.), 0023-4761, 24(3)

[36] Bublik, V. T., Karataev, V. V., Mil'vidskii, M. G., et al. (1979a). Defects in heavily doped with tin single crystals of InAs, Kristalografiya (Sov. Phys. Crystallogr.), 0023-4761, 24(5)

[37] Bubulac, L. O. (1988). Defects, diffusion and activation in ion implanted HgCdTe, J. Cryst. Growth., 0022-0248, 86(1-4)

[38] Bynin, M. A., & Matveev, Yu. A. (1985). Electronic structure of anion vacancies in indium arsenide, Sov. Phys. Semicond., 0015-3222, 19(11)

[39] Cai, L. C., Chen, H., , L., Huang, Q., & Zhou, J. M. (2003). Raman spectroscopic studies of InAs epilayers grown on the GaAs (001) substrates, J. Crystal Growth, ISSN 0022-0248, 253

[40] Capper, P., Elliot, C. T., & Eds, . (2001). Infrared Detectors and Emitters: Material and Devices, Kluwer Academic Publishers, 0-79237-206-9

[41] Capper, P. (1991). A review of impurity behavior in bulk and epitaxial $Hg_{1-x}Cd_xTe$, J. Vac. Sci. Technol. B, 0073-4211X., 9(3)

[42] Capper, P., Garland, J., & Eds, . (2011). Mercury Cadmium Telluride: Growth, Properties, and Applications, Wiley 2011, 978-0-47069-706-1

[43] Capper, P., & Ed, . (1994). Properties of Narrow Gap Cadmium-based Compounds, INSPEC, London, 0-85296-880-9

[44] Capper, P., & Ed, . (1997). Narrow-gap II-VI Compounds for Optoelectronic and Electromagnetic Applications, Chapman and Hall, London, 1997, 0-41271-560-0

[45] Casselman, T. N. (1981). Calculation of the Auger lifetime in p-type $Hg_{1-x}Cd_xTe$, J. Appl. Phys., 0021-8979, 52

[46] Casselman, T. N., & Petersen, P. E. (1980). A comparison of the dominant Auger transitions in p-type (Hg,Cd)Te, Solid State Commun., 0038-1098, 33

[47] Chen, H., Cai, L. C., Bao, C. L., Li, J. H., Huang, Q., & Zhou, J. M. (2000). Two-step method to grow InAs epilayer on GaAs substrate using a new prelayer, J. Crystal Growth, 0022-0248, 208(1-4)

[48] Cheung, D. T. (1985). An overview on defect studies in MCT, J. Vac. Sci. Technol., 0734-2101, A3(1)

[49] Chu, J., & Sher, A. (2008). Physics And Properties of Narrow Gap Semiconductors, Springer, 978-0-38774-743-9

[50] Chu, J., & Sher, A. (2010). Device Physics of Narrow Gap Semiconductors, Springer, 978-1-44191-039-4

[51] Fastow, R., Goren, D., & Nemirovsky, Y. (1990). Shockley-Read recombination and trapping in p-type HgCdTe, J. Appl. Phys., 0021-4651, 68(7)

[52] Dixit, A., Bansal, B., Venkataraman, V., Subbanna, G. N., Chandrasekharan, K. S., Arora, B. M., & Bhat, H. L. (2002). High-mobility InSb epitaxial films grown on a GaAs(001) substarte using liquid-phase epitaxy, Appl. Phys. Lett., 0003-6951, 80

[53] Dixit, V. A., Rodrigues, B. V., Venkataraman, R., Chandrasekharan, K. S., Chandrasekharan, K. S., Arora, B. M., & Bhat, H. L. (2002a). Growth of InSb epitaxial layer on GaAs(001) substrate by LPE and their characterizations, J. Cryst. Growth, 0022-0248, 235

[54] Dobbelaere, W., Boech, J., Heremans, R., et al. (1992). InAs p- n diodes grown on GaAs and GaAs-coated Si by molecular beam epitaxy, Appl. Phys. Lett, 0003-6951, 60(7)

[55] Eftekhari, G. (1997). The Effect of Sulfur Passivation and Rapid Thermal Annealing on the Properties of InAs MOS Structures with the Oxide Layer Deposited by Reactive Sputtering, Phys. Stat. Solidi (a), 0031-8965, 161(2)

[56] Egan, R. J., Tansley, T. L., & Chin, V. W. L. (1995). Growth of InAs from monoethyl arsine, J. Crystal Growth, 0022-0248, 147(1-2)

[57] Egemberdieva, S., Sh, , Luchinin, S. D., Saysenbaev, T., et al. (1982). Deep levels in the band gap of indium antimonide, Sov. Phys. Semicond., 0015-3222, 16(3)

[58] Esina, N. P., Zotova, N. V., Matveev, B. A., et al. (1985). Features of the luminescence of plastically deformed heterostructures of InAsSbP/ InAs, Sov. Phys. Semicond., 0015-3222, 19(11)

[59] Evstropov, V. V., Dzhumaeva, M., Zhilyaev, Yu. V., Nazarov, N., Sitnikova, A. A., & Fedorov, L. M. (2000). Dislocation origin and a model of the excessive tunnel current in GaP p-n structures, Semiconductors, 0015-3222, 34(11)

[60] Evstropov, V. V., Zhilyaev, Yu. V., Dzhumaeva, M., & Nazarov, N. (1997). Tunnel excess current in nondegenerated (p-n and m-s) silicon-containing III-V compound semiconductor structures, Semiconductors, 0015-3222, 31(2)

[61] Farrell, S., Rao, Mulpuri., Brill, G., Chen, Y., Wijewarnasuriya, P., Dhar, N., Benson, D., & Harris, K. (2011). Effect of Cycle Annealing Parameters on Dislocation Density Reduction for HgCdTe on Si, J. Electron. Mater., 0361-5235, 40(8)

[62] Fomin, I. A., Lebedeva, L. V., & Annenko, N. M. (1984). Investigation of deep levels in InAs using capacitance measurements of MIS structures, Sov. Phys. Semicond., 0015-3222, 18(4)

[63] Fowler, A. M., Gatley, I., Mc Intyre, P., Vrba, F. J., & Hoffman, A. (1996). ALADDIN, the 1024-1024 InSb array: design, description, and results, Proc.SPIE, 0027-7786X, 2816

[64] Fujisada, H., & Kawada, M. (1985). Temperature Dependence of Reverse Current in Be Ion Implanted InSb p+n Junctions, J. Appl. Phys., L76-L78, 0021-8979, 24

[65] Fukui, T., & Horikoshi, Y. (1979). Organometallic VPE Growth of InAs, Jpn. J. Appl. Phys., 1347-4065, 18

[66] Galkina, T. I., Penin, N. A., & Rassushin, V. A. (1966). Determination of the energy of the acceptor level of cadmium in indium arsenide, Sov.Phys. Solid State, 0367-3294, 8(8)

[67] Gao, H. H., Krier, A., & Scherstnev, V. V. (1999). High quality InAs growth by liquid phase epitaxy using gadolinium gettering, Semicond. Sci. Technol., 0268-1242, 14(3)

[68] Garland, J. M. B. E., Growth, of., Mercury, Cadmium., Telluride, pp.131-14., in, Mercury., cadmium, telluride., growth, properties., & applications, Capper. and, J. MBE Growth of Mercury Cadmium Telluride, in Mercury cadmium telluride: growth, properties, and applications, Capper, P. and Garland, J. (Eds.), Wiley, 978-0-47069-706-1, 131-149.

[69] Garland, J., & Sporken, R. (2011). Substrates for the Epitaxial Growth of MCT, in Mercury cadmium telluride: growth, properties, and applications, Capper, P. and Garland, J. (Eds.), Wiley, 978-0-47069-706-1, 75-94.

[70] Gelmont, B. L. (1978). Three-Band Kane Model of Auger Recombination, JETP (In Russia), N2, 536-544, 0044-4510, 75

[71] Gelmont, B. L. (1981). Auger Recombination in Narrow-Gap p-Type Semiconductor, Sov. Phys. Semicond., N7, 1316-1319, 0015-3222, 15

[72] Gelmont, B. L., & Sokolova, Z. N. (1982). Auger Recombination in Direct-Gap n-Type Semiconductors, Sov. Phys. Semicond., N9, 1670-1672, 0015-3222, 16

[73] Gelmont, B. L., Sokolova, Z. N., & Yassievich, I. N. (1982). Auger Recombination in Direct-Gap p-Type Semiconductors, Sov. Phys. Semicond., N3, 592-600, 0015-3222, 16

[74] Gheorghitse, E. I., Postolani, I. T., Smirnov, V. A., & Untila, P. G. (1989). Photoluminescence of p-InAs:Mn, Sov. Phys. Semicond.,0015-3222, 23(4)

[75] Golding, T. D., Holland, O. W., Kim, M. J., Dinan, J. H., Almeida, L. A., Arias, J. M., Bajaj, J., Shih, H. D., & Kirk, W. P. (2003). HgCdTe on Si: present status and novel buffer layer concepts, J. Electron. Mater., 0361-5235, 32(8)

[76] Golovanov, V. V., & Oding, V. G. (1969). The influence of deep-level compensation on the electrical properties of p-InSb, Sov. Phys. Semicond., 0015-3222, 3(2)

[77] Golovanov, V. V., Ivchenko, E. L., & Oding, V. G. (1973). Generation-recombination noise in p-InSb at 78 K, Sov. Phys. Semicond., 0015-3222, 7(4)

[78] Granato, A., & Lücke, K. (1956). Theory of Mechanical Damping Due to Dislocations, J. Appl. Phys.,0021-8979, 27(6)

[79] Guseinov, E. K., Ibragimov, R. I., Korotin, V. G., Nasledov, D. N., & Popov, Yu. G. (1971). The recombination processes in n-InSb in the temperature range 4.2- 77 K, Sov. Phys. Semicond., 0015-3222, 5(9)

[80] Guseinov, E. K., Mikhailova, M. P., Nasledov, D. N., et al. (1969). Impurity photoconductivity in InAs, Sov. Phys. Semicond.,0015-3222, 3(11)

[81] Guseva, M. I., Zotova, N. V., Koval', A. V., & Nasledov, D. N. (1975). Radiative recombination in indium arsenide implanted with Group IV elements, Sov. Phys. Semicond.,0015-3222, 9(5)

[82] Halt, D.B. and Yacobi, G.Ya(2007). Structural Defects in Semiconductors. Electronic Properties, Device Effects and Structures, Cambridge University Press, 0-52181-934-2

[83] Haywood, S. K., Martin, R. W., Mason, N. J., & Walker, P. J. (1990). Growth of InAs by MOVPE using TBAs and TMIn, J. Electron. Mater., 0361-5235, 19(8)

[84] He, W., & Celik-Batler, Z. (1996). f noise and dark current components in HgCdTe MIS infrared detectors, Solid-State Electron., 0038-1101, 19(1)

[85] Hoffman, A. W., & Randall, D. (1991). High-performance 256 x 256 InSb FPA for astronomy, Proc. SPIE, 0027-7786X., 1540

[86] Hollis, J. E. L., Choo, S. C., & Heasell, E. L. (1967). Recombination center in InSb, J. Appl. Phys., 0021-8979, 38(4)

[87] Holmes, D. E., & Kamath, G. S. (1980). Growth-characteristics of LPE InSb and InGaSb, J. Electron. Mater., 0361-5235, 9

[88] Holt, D. B., & Yacobi, B. G. (2007). Extended defects in Semiconductors. Electronic Properties, Device Effects and Structures, Cambridge University Press, 978-0-52181-934-3

[89] Huang, K. T., Hsu, Y., Cohen, R. M., & Stringfellow, G. B. (1995). OMVPE growth of InAsSb using novel precursors, J.Crystal Growth, 0022-0248, 156(4)

[90] Hulme, K. F., & Mullin, J. B. (1962). Indium Antimonide-A review of its Preparation, Properties and Device Applications, Solid-State Electron., 0038-1101, 5

[91] Hurwitz, C. E., & Donnelly, J. P. (1975). Planar InSb Photodiodes Fabricated by Be and Mg Ion Implantation, Solid State Electron., 0038-1101, 18

[92] Iglitsyn, M. I., & Solovyov, E. (1968). Determination of the ionization energy of cadmium in indium arsenide, Sov. Phys. Semicond.,0015-3222, 2(7)

[93] Ilyenkov, J. A., Kovalevskaya, T. E., & Kovchavtsev, A. P. (1992). Estimation of the parameters of deep levels in MIS structures based on InAs, Poverhnost: fizika, himiya, mehanika (In Russia), 0734-1520, 1(1), 62-69.

[94] Ismailov, N. M., Nasledov, D. N., & Smetannikova, Y. S. (1969). The impurity photoconductivity of indium antimonide at low temperatures, Sov. Phys. Semicond.,, 2(6)

[95] Ivasiv, Z. F., Sizov, F., & F.and, Tetyorkin. V. V. (1999). Noise spectra and dark current investigations n^+-p type $Hg_{1-x}Cd_xTe$ (x0.22) photodiodes, Semicond. Phys. Quant. Electron. Optoelectron. (Kiev), 1605-6582, 2(3)

[96] Johnson, S. M., Rhiger, D. R., Rosbeck, J., Peterson, P., , J. M., Taylor, S. M., & Boyd, M. E. (1992). Effect of dislocations on the electrical and optical properties of long-wavelength infrared HgCdTe photovoltaic detectors, J. Vac. Sci. Technol. B, 0734-2101, 10

[97] Jones, C. E., Nair, V., Lindquist, J., & Polla, D. L. (1982). Effects of deep-level defects in $Hg_{1-x}Cd_xTe$ provided by DLTS, J. Vac. Sci. Technol. 0734-2101, 21(1)

[98] Jóźwikowska, A., Jóźwikowski, K., Rutkowski, J., Orman, Z., & Rogalski, A. (2004). Generation-recombination effects in high temperature HgCdTe heterostructure photodiodes, Opto-Electron. Rev., 1230-3402, 12(4)

[99] Kalem, S., Chyi-I, J., Morkoç, H., Bean, R., & Zanio, K. (1998). Growth and transport properties of InAs epilayers on GaAs, Appl. Phys. Lett., 0003-6951, 53(17)

[100] Karataev, V. V., Nemtsova, G. A., Rizhova, N. S., & Yugova, T. G. (1977). Effect of heat treatment on the electrical properties of undoped indium arsenide, Sov. Phys. Semicond., 0015-3222, 11(9)

[101] Kazaki, K., Yahata, A., & Miyao, W. (1976). Properties of InSb Photodiodes Fabricated by Liquid Phase Epitaxy, J. Appl. Phys., 0021-8979, 15

[102] Kesamanly, F. P., Lagunova, T. S., Nasledov, D. N., et al. (1968). Electrical properties of p-type indium arsenide crystals, Sov. Phys. Semicond., 0015-3222, 2(1)

[103] Kevorkov, M. N., Popkov, A. N., Uspensky, V. S., et al. (1980). Thermal acceptors in indium antimonide, Izv. Akad. Nauk SSSR, Neorg. Mater. (In Russia), 0000-2337X., 16(12)

[104] Kimukin, I., Biyikli, N., & Ozbay, E. (2003). InSb high-speed photodetectors grown on GaAs substrate, J. Appl. Phys., 94, 0021-8979, 15(15), 5416-5414.

[105] Kinch M.A.(1981). Metal-insulator semiconductor infrared detectors, in Semiconductor and Semimetals, Willardson, R.K. and Beer, A.C. (Eds.), New York: Academic Press, ch.7, 978-0-12752-118-3, 18

[106] Kornyushkin NA, NA Valisheva, Kovchavtsev AP, GL Kuryshev(1996). Influence of the interface and deep levels in the forbidden gap on the capacitance-voltage characteristics of InAs MIS structures, Semiconductors.,0015-3222, 30(5)

[107] Korotin, V. G., Krivonogov, S. N., Nasledov, D. N., & Smetannikova, Y. S. (1976). The model of recombination processes in n-InSb, Sov. Phys. Semicond., 0015-3222, 10(1)

[108] Kosogov, O. V., & Perevyaskin, L. S. (1970). Electrical Properties of Epitaxial p+-n Junctions in Indium Antimonide, Sov. Phys. Semicond., 0015-3222, 8

[109] Kozlowski, L., Vural, K., Luo, J., Tomasini, A., Liu, T., & Kleinhans, W. K. (1999). Low-noise infrared and visible focal plane arrays, Opto-Electron. Rev., 1230-3402, 7

[110] Krishnamurthy, S., Berding, M. A., Robinson, H.and., & Sher, A. (2006). Tunneling in long-wavelength infrared HgCdTe photodiodes, J. Electron. Mater., 0361-5235, 35(6)

[111] Kuan, C. H., Lin, R. M., Tang, S. F., & Sun, T. P. (1996). Analysis of the Dark Current in the Bulk of InAs Diode Detectors, J. Appl. Phys., 0021-8979, 80

[112] Kumagawa, M., Witt, A. F., Lichtenstelger, M., & Gatos, H. C. (1973). Current-controlled and dopant modulation in liquid phase epitaxy, J. Electrochem. Soc., 0013-4651, 120

[113] Kuryshev, G. L., Kovchavtsev, A. P., & Valisheva, N. (2001). Electronic properties of MIS structures based on InAs, Semiconductors, 0015-3222, 35(9)

[114] Kuryshev, G. L., Lee, I. I., Bazovkin, V. M., et al. (2009). Threshold parameters of multielement InAs hybrid IR FPA and InAs-based devices, Prikladnaya Fizika (In Russia), 1996-0948, 2(2), 79-92.

[115] Kuze, N., Camargo, E. G., Ueno, K., et al. (2007). High performance miniaturized InSb photovoltaic infrared sensors operating at room temperature, J. Crystal Growth, 0022-0248, 301-302

[116] Kveder, V., Kittler, M., & Schröter, W. (2001). Recombination activity of contaminated dislocations in silicon: A model describing electron-beam-induced current contrast behavior, Phys. Rev.B, 0163-1829, 63

[117] Kveder, V. V., Labusch, R., & Ossipyan, Yu. A. (1985). Frequency dependence of the dislocation conduction in Ge and Si, Phys. Stat. Sol., 0370-1972, 92

[118] Labusch, R. (1982). One dimensional transport along dislocations, Physica, 0921-4526, 117B-118B(1)

[119] Labusch, R., & Schröter, W. (1983). Electrical Properties of Dislocations in Semiconductors, in Dislocations in Solids, Nabarro, F.R.N. (ed.), Amsterdam: North-Holland, 0-44485-050-3, 5

[120] Laff R.A. and Fan H.Y.(1961). Carrier lifetime in indium antimonide, Phys. Rev., , 121(1)

[121] Liang, S. (1966). Preparation of Indium Antimonide, in Compound Semiconductors, Willardson, R.K. and Georing, H.L. (Eds.), N.Y., 227-237.

[122] Lin, R. M., Tang, S. F., Lee, S. C., Kuan, C. H., Chen, G. S., Sun, T. P., & And, Wu. J. C. (1997). Room Temperature Unpassivated InAs p-i-n Photodetectors Grown by Molecular Beam Epitaxy, IEEE Trans. Electron Dev., 0018-9383, 44

[123] Litter, C. L., Seiler, D. G., & Loloee, M. R. (1990). Magneto-optical investigations of impurity and defect levels in HgCdTe alloys, J. Vac. Sci. Technol.A, 0734-2101, 8(2)

[124] Liu, W. K., Winesett, J., Weiluan, Xuemei., Zhang, Santos. M. B., Fang, X. M., & Mc Cann, P. J. (1997). Molecular beam epitaxy of InSb on Si substrates using fluoride buffer layers, J. Appl. Phys., 0021-8979, 81(4)

[125] Lopes, V. C., Syllaios, A. J., & Chen, M. C. (1993). Minority carrier lifetime in mercury cadmium telluride, Semicond. Sci. Technol., 0268-1242, 8(2)

[126] Madejczyk, P., Piotrowski, A., Gawron, W., Klos, K., Pawluczyk, J., Rutkowski, J., Piotrowski, J., , J., & Rogalski, A. (2005). Growth and properties of MOCVD HgCdTe epilayers on GaAs substrates, Opto-Electron. Rev., 1230-3402, 13(3)

[127] Madelung, O. (1996). Semiconductors-Basic Data, 2nd revised Edition, Springer, 3-54060-883-4

[128] Madelung, O., Rössler, U., Schulz, M. ., & Eds, . (2003). Landolt-Börnstein- Group III Condensed Matter. Numerical Data and Functional Relationships in Science and Technology, Impurities and Defects in Group IV Elements, IV-IV and III-V Compounds. Part b: Group IV-IV and III-V Compounds, Springer, 978-3-54043-086-5, 41A2b

[129] Mahony, J., & Maseher, P. (1977). Position- annihilation study of vacancy defects in InAs, Phys. Rev. B., 1997, 0015-3222, 55(15)

[130] Maier, H., & Hesse, J. (1980). Growth, properties and applications of narrow-gap semiconductors, in Crystall Growth Properties and Applications, Freyhard, H.C. (Ed.), Springer Verlag, Berlin, , 145-219.

[131] Malyutenko, V. N., Bolgov, S. S., Pipa, V. I., & Chaykin, V. I. (1980). Quantum yield of recombination radiation in n-InSb, Sov. Phys. Semicond., N4, 781-786, 0015-3222, 14

[132] Maranowski, K. D., Peterson, J. M., Johnson, S. M., Varesi, J. B., Radford, W. A., Chields, A. C., Bornfreund, R. E., & Buell, A. A. (2001). MBE growth of HgCdTe on silicon substrates for large format MWIR focal plane arrays, J. Electron. Mater., 0361-5235, 30

[133] Matare, H. F. (1971). Defect Electronics in Semiconductors, Wiley, ISBN , 13, 978-0471576181.

[134] Maxey, C. D. (2011). Metal-Organic Vapor Phase Epitaxy (MOVPE) Growth, in Mercury cadmium telluride: growth, properties, and applications, Capper, P. and Garland, J. (Eds.), Wiley, 978-0-47069-706-1, 113-129.

[135] Mc Nall, P. J. (1970). Ion Implantation in InAs and InSb, in Radiation Effects and Defects in Solids, 16747348, 6

[136] Mengailis, I., & Calawa, A. R. (1966). Solution regrowth of planar InSb lase structure, J. Electrochem. Soc., 0013-4651, 113

[137] Micklethwaite, W. F. M., & Johnson, A. J. (2000). InSb: materials and devices, in Infrared Detectors and Emitters: Materials and Devices, Capper, P. and Elliott, C.T. (Eds.), Kluwer Academic Publishers, Boston, 978-0-79237-206-6, 177-204.

[138] Milnes A.G.(1973). Deep impurities in semiconductors, Wiley, 0-47160-670-7

[139] Mozzi, R. L., & Lavine, J. M. (1970). Zn-Diffusion Damage in InSb Diodes, J. Appl. Phys., 0021-8979, 41

[140] Mroczkowski, J. A., Shanley, J. F., Reine, M. B., Lo, Vecchio. P., & Polla, D. L. (1981). Lifetime measurement in Hg0.7Cd0.3Te by population modulation, Appl. Phys. Lett., 0003-6951, 38(4)

[141] Nasledov, D. N., & Smetannikova, Y. S. (1962). Temperature dependence of the lifetime of carriers in indium antimonide, Sov. Phys. Solid State, 0367-3294, 4(1)

[142] Nemirovsky, Y., & Unikovsky, A. (1992). Tunnelling and 1/f noise currents in HgCdTe photodiodes, J. Vac. Sci. Technol. B., 0734-2101, 10(4)

[143] Nemirovsky, Y., Fastow, R., Meyassed, M., & Unikovsky, A. (1991). Trapping effects in HgCdTe, J.Vac.Sci.Technol. B., 0734-2101, 9(3)

[144] Nemirovsky, Y., Rosenfeld, D., Adar, R., & Kornfeld, A. (1989). Tunneling and dark currents in HgCdTe photodiodes, J.Vac.Sci.Technol. A, 0734-2101, 7(2)

[145] Nishitani, K., Nagahama, K., & Murotani, T. (1983). Extremely Reproducible Zinc Diffusion into InSb and Its Application to Infrared Detector Array, J. Electron. Mater., 0361-5235, 12(1)

[146] Nitccki, R., Pohoryles, B., & (1985, . (1985). Tunneling from dislocation cores in silicon Schottky diodes, Appl. Phys., 0947-8396, A36

[147] Norton, P. (2002). HgCdTe infrared detectors, Opto-Electron. Rev., 1230-3402, 10(3)

[148] Norton, P. R. (1999). Infrared detectors in the next millennium, Proc.SPIE, 0027-7786X., 3698

[149] Omel'yanovskii, E. M., Fistul', V. I., Balagurov, L. A., et al. (1975). On the behavior of transition-metal impurities in III-V compounds, Sov. Phys. Semicond., 0015-3222, 9(3)

[150] Osipiyan, Yu. A., & Savchenko, I. B. (1968). Experimental observation of the influence of light on plastic deformation of cadmium sulphide, JETP Letters (In Russia), 0021-3640, 7

[151] Ozer, S., & Besikci, C. (2003). Assessment of InSb photodetectors on Si substrates, J. Phys. D: Appl. Phys., 0022-3727(5)

[152] Parker, S. G., Willson, O. W., & Barbel, B. H. (1965). Indium antimonide of high perfection, J. Electrochem. Soc., 0013-4651, 112

[153] Parrish, W. J., Blackwell, J. D., Kincaid, G. T., & Paulson, R. C. (1991). Low-cost high-performance InSb 256 x 256 infrared camera, Proc. SPIE, 0027-7786X., 1540

[154] Partin, D. L., Green, L., Morelli, D. T., Heremans, J., Fuller, B. K., & Thrush, C. M. (1991). Growth and characterization of indium arsenide thin films, J. Electron. Mater., 0361-5235, 20(12)

[155] Pehek, J., & Levinstein, H. (1965). Recombination radiation from InSb. Phys. Rev., , 140(2), 576-586.

[156] Petersen, P. E. (1970). Auger Recombination in $Hg_{1-x}Cd_xTe$, J. Appl. Phys., 0021-4922, 41

[157] Petersen, P. E. (1981). Auger Recombination in Mercury Cadmium Telluride, in Semiconductors and Semimetals, Willardson, R.K. and Beer A.C. (Eds.), Academic Press, 978-0-12752-118-3, 18

[158] Peterson, J. M., Franklin, J. A., Readdy, M., Johnson, S. M., Smith, E., Radford, W. A., & Kasai, I. (2006). High-quality large-area MBE HgCdTe/Si, J. Electron. Mater., 0361-5235, 36

[159] Plitnikas, A., Krotkus, A., & Dorovolskis, Z. (1982). The current-voltage characteristics of compensated indium arsenide in strong electric fields, Sov. Phys. Semicond., 0015-3222, 16(6)

[160] Polla, D. L., & Jones, C. E. (1981). Deep level studies of $Hg_{1-x}Cd_xTe$. I: Narrow-band-gap space-charge spectroscopy, J. Appl. Phys., 0021-8979, 52(8)

[161] Polla, D. L., Aggarwal, R. L., Mroczkowski, J. A., Shanley, J. F., & Reine, M. B. (1982). Observation of deep levels in $Hg_{1-x}Cd_xTe$ with optical modulation spectroscopy, Appl. Phys. Lett., 0003-6951, 40(4)

[162] Polla, D. L., Reine, M. B., & Jones, C. E. (1981a). Deep level studies of $Hg_{1-x}Cd_xTe$. II: Correlation with photodiode performance, J. Appl. Phys., 0021-8979, 52(8)

[163] Polla, D. L., Tobin, S. P., Reine, M., & B.,and, Sood. A. K. (1981b). Experimental determination of minority-carrier lifetime and recombination mechanisms in p-type $Hg_{1-x}Cd_xTe$, J. Appl. Phys., 0021-8979, 52(8)

[164] Razeghi, M. (2003). Overview of antimonide based III-V semiconductor epitaxial layers and their applications at the center for quantum devices, Eur. Phys. J. Appl. Phys. 1286-0042, 23

[165] Reine, M. B. (2000). Photovoltaic detectors in MCT, In Infrared Detectors and Emitters: Materials and Devices, P.Capper and C.T. Elliott, Eds., Kluwer Academic Publishers, Boston, 0-79237-206-9

[166] Rogalski, A. (2009). Infrared detectors for the future, Acta Physica Polonica A, 0587-4246, 116(3)

[167] Rogalski, A. (2011). Infrared Detectors, 2nd ed., CRC Press, 978-1-42007-671-4

[168] Rogalski, A., Adamiec, K., & Rutkowski, J. (2000). Narrow-Gap Semiconductor Photodiodes, SPIE Press, Bellingham, 0-81943-619-4

[169] Rogalski, A., & Ed, . (1995). Infrared Photon Detectors, SPIE Optical Engineering Press, 081941798

[170] Rosbeck, J. P., Kassi, I., Hoendervoog, R. M., & Lanir, T. (1981). High Performance Be Implanted InSb Photodiodes, IEEE IEDM, 1074-1879, 81

[171] Rosenfeld, D., & Bahir, G. (1992). A model for the trap-assisted tunnelling mechanism in diffused n-p and implanted n^+-p HgCdTe photodiodes, IEEE Trans. Electron. Dev., 0018-9383, 39(7)

[172] Schaake, H. R. (1985). The existence region of the $Hg_{0.8}Cd_{0.2}Te$ phase field, J. Electron. Mater., 0361-5235, 14(5)

[173] Schaake, H. R., Tregilgas, J. H., Lewis, A. J., & Everett, M. (1983). Lattice defects in (Hg,Cd)Te: Investigations of their nature and evolution, J. Vac. Sci. Technol. A, 0734-2101, 1(3)

[174] Seibt, M., Halil, R., Kveder, V.and., & Schröter, W. (2009). Electronc states at dislocations and metal silicide precipitates in crystalline silicon and their role in solar cell materials, J. Appl. Phys A, 0021-8979, 96

[175] Shaw, D., & Capper, P. (2011). Extrinsic Doping, in Mercury cadmium telluride: growth, properties, and applications, Capper, P. and Garland, J. (Eds.), Wiley, 978-0-47069-706-1, 317-337.

[176] Shepelina, O. S., & Novototsky-Vlasov, Y. F. (1992). Equilibrium parameters of deep levels in bulk indium antimonide, Semiconductors, 0015-3222, 26(6)

[177] Sher, A., Berding, M. A., van Schilfgaarde, M., & Chen-Ban, An. (1991). HgCdTe status review with emphasis on correlations, native defects and diffusion, Semicond. Sci. Technol., C59-C70, 0268-1242, 6

[178] Shikin, V. B., & Shikina, Yu. V. (1995). Charged dislocations in semiconductors, Physics-Uspekhi (Advances in Physical Sciences), In Russia, 0042-1294, 38(8)

[179] Shin, S. H., Arias, J. M., Edwall, D. D., Zandian, M., Pasko, J. G., & De Wammes, R. E. (1992). Dislocation reduction in HgCdTe in GaAs and Si, J. Vac. Sci. Technol. B, 0022-5355, 10

[180] Shin, S. H., Arias, J. M., Zandian, M., Pasko, J. G., & De Wames, R. E. (1991). Effect of the dislocation density on minority-carrier lifetime in molecular beam epitaxial HgCdTe, Appl. Phys. Lett., 0003-6951, 59

[181] Sipovskaya, M. A., Smetannikova, Y. S., & (1984, . (1984). The dependence of the carrier lifetime on the electron density in n-InSb, Sov. Phys. Semicond., 0015-3222, 18(2)

[182] Strelnikova, I. A., Ermakov, N. G., Laptev, A. V., & Rauhman, M. R. (1993). Effect of heat treatment on the properties of indium antimonide, Inorg. Mater. (In Russia), 0000-2337X., 29(3)

[183] Sukach, A., Tetyorkin, V., Olijnyk, G., Lukyanenko, V., & Voroschenko, A. (2005). Cooled InAs photodiodes for IR applications, Proc. SPIE., 0027-7786X., 5957

[184] Sukach A.V. and Tetyorkin V.V.(2009). Ultrasonic treatment-induced modification of the electrical properties of InAs p-n junctions, Tech. Phys. Lett., N6, 514-517, 1063-7850, 36

[185] Sukach, A., Tetyorkin, V., Olijnuk, G., Lukyanenko, V., & Voroschenko, A. (2005). Cooled InAs photodiodes for IR applications, Proc. SPIE, 0027-7786X., 5957

[186] Sze, S. M. (1981). Physics of Semiconductor Devices, second edition, Wiley, N.Y. 0-47105-661-8

[187] Tetyorkin, V., Sukach, A., & Tkachuk, A. (2011). InAs Infrared Photodiodes, in Advances in Photodiodes, Dalla Betta, G-F. (ed.), Intech Open Acces Publisher, 978-9-53307-163-3

[188] Tregilgas, J. H., Polgreen, T. L., & Chen, M. C. (1988). Dislocations and electrical characteristics of HgCdTe, J. Crystal Growth, 0022-0248, 86(1-4)

[189] Tribolet, P., Chorier, P., & Pistone, F. (2003). Key performance drivers for coded large IR staring arrays, Proc. SPIE, 0027-7786X., 5074

[190] Trifonov, V. I., & Yaremenko, N. G. (1971). The deep donor level in n-InSb, Sov. Phys. Semicond., 0015-3222, 5(5)

[191] Tsitsina, N. P., Fadeeva, A. P., Vdovkina, E. E., et al. (1975). Effect of low-temperature annealing on the properties of InSb, Izv. Akad. Nauk SSSR, Neorg. Mater (In Russia), 0000-2337X., 11(5)

[192] Valyashko, E. G., Pleskacheva, T. B., & Tyapkina, N. D. (1975). Effect of heat treatment on electrical properties and impurity photoconductivity of p-InSb, Izv. Akad. Nauk SSSR, Neorg. Mater., (In Russia), 0000-2337X., 11(6)

[193] Volkov, A. S., & Golovanov, V. V. (1967). Recombination processes in p-InSb, Sov. Phys. Semicond., 0015-3222, 1(2)

[194] von-Streiber, Eichel., , C., Behet, M., Heuken, M., & Heime, K. (1997). Doping of InAs, GaSb and InPSb by low pressure MOVPE, J. Crystal Growth, 0022-0248, 170(1-4)

[195] Voronina, T. I., Lagunova, T. S., Kizhaev, S. S., et al. (2004). Growth and magnesium doping of InAs layers by vapor-phase epitaxy from organometallic compounds, Semiconductors, 0015-3222, 38(5)

[196] Voronina, T. I., Lagunova, T. S., Moiseev, K. D., et al. (1999). Electrical properties of epitaxial indium arsenide and narrow-gap solid solutions on its base, Semiconductors, 0015-3222, 33(7)

[197] Voronina, T. I., Zotova, N. V., & Kizhaev, S. S. (1999a). Fluorescent and other properties of InAs layers and p-n-structures on their base, grown by vapor-phase epitaxy from organometallic compounds, Semiconductors, 0015-3222, 33(10)

[198] Vydyanath, H. R. (1981). Lattice Defects in Semiconducting $Hg_{1-x}Cd_xTe$ Alloys, J. Electrochem. Soc., 0013-4651, 128(12)

[199] Vydyanath, H. R. (1991). Mechanisms of incorporation of donor and acceptor dopants in (Hg,Cd)Te alloys, J. Vac. Sci. Technol. B, 0734-2101, 9

[200] Wang, J. Y. (1980). Effect of trap tunneling on the performance of long-wavelength $Hg_{1-x}Cd_xTe$ photodiodes, IEEE Trans. on Electron Dev., 0018-9383, ED-27(1)

[201] Watkins, S. P., Tran, C. A., Ares, R., & Soerensen, G. (1995). High mobility InAs grown on GaAs substrates using tertiarybutyl arsine and trimethylindium, Appl. Phys. Lett., 0003-6957, 66(7)

[202] Whelan, M. (1969). Leakage currents of n/p silicon diodes with different amounts of dislocations, Solid-State Electronics, 0038-1101, 12(6)

[203] Wimmers, J. T., & Smith, D. S. (1983). Characteristics of InSb photovoltaic detectors at 77 K and below, Proc.SPIE, 0027-7786X., 364

[204] Wimmers, J. T., Davis, R. M., Niblack, C. A., & Smith, D. S. (1988). Indium antimonide detector technology at Cincinnati Electronics Corporation, Proc.SPIE, 0027-7786X., 930

[205] Yamamoto, T., Miyamoto, Y., & Tanikawa, K. (1985). Minority carrier lifetime in the region close to the interface between the anodic oxide CdHgTe, J. Crystal Growth, 0022-0248, 72(1)

[206] Yang, J., Yu, Z., & Tang, D. (1985). The defects in $Hg_{0.8}Cd_{0.2}Te$ annealed at high temperature, J. Crystal Growth, 0022-0248, 72(1-2)

[207] Yano, M., Nogami, M., Matsuchima, Y., & Kimata, M. (1977). Molecular beam epitaxial growth of InAs, Japan. J. Appl. Phys., 0021-4922, 16(12)

[208] Yonenaga, I. (1998). Dynamic behavior of dislocations in InAs: in comparison with III-V compounds and other semiconductors, J. Appl. Phys., 0021-4922, 84

[209] Zaitov, F. A., Gorshkov, O. V., Polyakov, A. Y., et al. (1981). The nature of deep acceptors in indium antimonide, Sov. Phys. Semicond., 0015-3222, 15(6)

[210] Zitter, R. N., Strauss, A. J., & Attard, A. E. (1959). Recombination processes in p-type indium antimonide, Phys. Rev., , 115(2)

[211] Zotova, N. V., Karataev, V. V., & Koval', A. V. (1975). Photoluminescence of n-InAs crystals doped with tin, Sov. Phys. Semicond.,0015-3222, 9(10)